DOE/NASA CONTRACTOR REPORT

DOE/NASA CR-161856

PERFORMANCE EVALUATION OF THE SOLAR KINETICS T-700 LINE CONCENTRATING SOLAR COLLECTOR

Prepared from documents furnished by

Wyle Laboratories
7800 Governors Drive West
Huntsville, Alabama 35807

Under Contract DEN8-000006

Monitored by

National Aeronautics and Space Administration
George C. Marshall Space Flight Center, Alabama 35812

For the U. S. Department of Energy

(NASA-CR-161856) PERFORMANCE EVALUATION OF THE SOLAR KINETICS T-700 LINE CONCENTRATING SOLAR COLLECTOR Final Report (Wyle Labs., Inc.) 49 p HC A03/MF A01 CSCL 10A

N82-10502

Unclas
G3/44 27716

U.S. Department of Energy

Solar Energy

TABLE OF CONTENTS

TABLE OF CONTENTS (Continued)

1.0 PURPOSE

The purpose of this document is to present the test procedures used and the test results obtained during an evaluation test program. The test program was conducted to obtain performance data for the Solar Kinetics, Inc., T-700 line concentrating parabolic trough collector. All tests took place at the Marshall Space Flight Center Solar Test Facility. The test was conducted and the data evaluated using the methods provided in References 2.1, 2.2, 2.3, and 2.4 as applicable

2.0 REFERENCES

2.1	MTCP-DC-SHAC-426	Test Procedure for Performance Evaluation of the Solar Kinetics Solar Concentrating Collector
2.2	ASHRAE 93-77	Methods of Testing to Determine the Thermal Performance of Solar Collectors
2.3	Solar Kinetics	Solar Collectors for Process Heat up to 650°
2.4	Transactions of the ASME 16/Vol. 120 Feb. 1980	Incident-Angle Modifier and Average Optical Efficiency of Parabolic Trough Collectors

3.0 COLLECTOR DESCRIPTION

3.1 Manufacturer: Solar Kinetics, Inc.

Manufacturer's Address: 8120 Chancellor Tow
Dallas, Texas 75247
214/630-9328

3.2 Specifications:

Type:	Line Focus Concentrating Collector
Working Fluid:	Liquid (Therminol 44)
Receiver:	The black chrome plated steel receiver tube is covered by a stagnant air annulus Pyrex glass tubing
Reflector:	The parabolic contoured aluminum mirror surface is covered with metallized acrylic film FEK 244
Array Length:	82' 11½"
Array Width:	7' 2½"
Module Width:	7' 2½"

3.0 COLLECTOR DESCRIPTION (Continued)

3.2 Specifications (Continued)

Module Length:	20' ½"
Mirror Width:	7'
Mirror Length:	19' 11 3/4"
Reflectance:	.84
Max. Vertical Height:	102"
Rotation Axis Height:	57"
Tracking Angle:	270°
Stow Angle:	45°
System Weight:	4 lb/ft^2
Receiver Tube:	1.625 O.D.
Annulus Medium	Stagnant air
Selective Surface:	Black chrome
Absorptivity:	.94 - .97
Emissivity:	.18 @ 500°F
Receiver Cover:	Pyrex glass
Max. Operating Temperature:	650°
Max. Operating Pressure:	250 psi.
Properties of Working Fluid:	$\gamma = 7.9927 - .00373\ T_f$ lb/gal
	$C_p = .4425 + .00033\ T_f$ Btu/lbm°F
	T_f: fluid inlet temperature

4.0 SUMMARY

Thermal performance tests were conducted for the Solar Kinetics T-700 line concentrating solar collector at the Marshall Space Flight Center Solar Test Facility. Four modules, each one 7' x 20', connected in series were mounted horizontally in a north-south orientation to track the sun from east to west. The collector array was driven by a single drive mechanism which is controlled by an electronic tracking device. Pyranometers which measure the total and diffused components of the solar radiation were mounted on the collector plane to track with the collector.

A high temperature fluid supply loop was designed and constructed for the test. A schematic of this test loop is shown in Figure 1. Relevant test conditions and the data obtained during the test program are listed in Tables I through IV for the thermal performance tests. Table V and Table VI are the collector tracking angles and tracking speed respectively on the 21st day of each month. In addition, graphic presentations of data obtained from the thermal performance tests are shown in Figure 2 through 8. Figures 9 and 10 show the typical solar radiation measured on the collector tracking plane. Figures 11 and 12 show the results of the collector return line and collector receiver tube heat loss tests. Figure 13 is the comparison of efficiency derived from the collector heat loss test with the normal thermal performance test, verifying the results of the thermal performance tests. Figures 14 and 15 show the collector tracking accuracy versus the sky conditions (clear, intermittent, and cloudy). Figures 16 and 17 show the collector performance versus the sky conditions.

5.0 TEST CONDITIONS AND TEST EQUIPMENT

5.1 Ambient Conditions

Unless otherwise specified herein, all tests were performed at ambient conditions immediately surrounding the collector at the MSFC solar testing site at the time of test.

5.2 Instrumentation and Equipment

All test equipment and instrumentation used in the performance of this test program comply with the requirement of MSFC-MMI-5300.4C, Metrology and Calibration. Testing took place at the MSFC Solar Test Bed Facility. A listing of equipment used for testing follows:

Appartus	Manufacturer/Model	Range/Accuracy
Data Logger	Model 2240A John Fluke Company	Multi-range Thermocouples
Thermocouple	Med-Therm Inc.	-300°F - 400°F/±.5°F
Pyranometer	Eppley PSP	0 - 800 Btu/hr.ft.^{2}/Class 1
Flow Meter	Potter	0 - 19 GPM/±0.2 GPM
Liquid Loop	Designed and Assembled at MSFC	1 ~ 12 GPM

6.0 TEST REQUIREMENTS AND PROCEDURES

6.1 Collector Time Constant Test

6.1.1 Requirement

The collector time constant shall be determined by abruptly reducing the solar flux to zero. This will be done with the inlet temperature holding at 140°F, while the liquid is flowing at approximately 10 gal/min.

The differential temperature across the collector shall be monitored to determine the time required to reach the condition of:

$$\frac{\Delta T(t)}{\Delta Ti} = .368$$

where $\Delta T(t)$ is the differential temperature at time t after the solar flux is reduced to zero and ΔTi is the differential temperature prior to the reduction of solar flux.

The following data will be recorded for the test:

(1) Solar flux.
(2) Ambient temperature.
(3) Inlet fluid temperature.
(4) Outlet fluid temperature.
(5) Liquid flow rate.

6.1.2 Procedure

1. Set the collector on tracking mode.

2. Adjust the fluid flow rate to 10 gal/min.

3. Adjust the inlet temperature to 140°F.

4. Monitor collector inlet and outlet temperature.

5. When the inlet and outlet temperature stabilized, switch the collector back to stow position.

6. Record the change of ΔT across the collector.

6.1.3 Results

The results of the time constant test is shown in Figure 2. The time constant for this collector with Therminol 44 as heat transfer fluid is approximately 58 seconds for 4 collector modules in series. Table I is the listing of data recorded during the time constant test.

6.0 TEST REQUIREMENTS AND PROCEDURES (Continued)

6.2 Collector Tracking Performance Test

6.2.1 Requirement

Accurate tracking of a concentrating collector is critical to its performance. The purpose of this test is to examine the effect of tracking error on the collector efficiency. This will be done by manually moving the collector out of track to a fixed position ahead of the sun. Then, let the sun pass over the receiver tube while maintaining the inlet fluid to the collector at a constant temperature. As the sun moves toward focusing the solar ray starts to intercept the receiver tube, and the outlet temperature begins to increase until the sun is fully focused, then it begins to decrease when the sun starts to move away from focusing.

The following data will be recorded for the test:

(1) Solar flux.
(2) Ambient temperature.
(3) Inlet fluid temperature.
(4) Outlet fluid temperature.
(5) Liquid flow rate.
(6) Collector set angle.

6.2.2 Procedures

1. Manually rotate the collector toward the west past the sun. Hold and record the collector angle at this position.

2. Maintain the inlet fluid at a constant temperature.

3. Monitor the collector inlet and outlet temperature while the sun is moving across the receiver tube.

6.2.3 Results

Several tests were performed and the results were superimposed into one graph. Figure 3 shows the collector efficiency versus the angle of off tracking. The inlet temperature for all tests were maintained at 150°F. Table VI showed that the collector tracking speed is not constant during the day. Therefore, the scattering of Figure 3 can be reduced if the efficiency is plotted versus the angle of off tracking. An off tracking of one degree will cause the efficiency to drop from 55% to 45%. Therefore, tracking accuracy tolerance shall be within .25 degrees. A shaft encoder was installed on the collector so that the collector position can be monitored. These collector position data were used to compare with the theoretical calculation of the collector position angles to determine the collector tracking performance. Detailed calculation method will be presented in the next Section. Figure 14 showed the SKI tracker performance during a clear day. The tracker was able to track the sun accurately (within .25 degrees). Figure 15

6.0 TEST REQUIREMENTS AND PROCEDURES (Continued)

6.3 Collector Thermal Efficiency Test

6.3.1 Test Requirement

Thermal performance data from the Solar Kinetics, Inc. line concentrating collector T-700 shall be obtained at the MSFC outdoor test bed facility under natural environment conditons. Because of its high temperature application, Therminol 44 will be used as heat transfer fluid. The collector shall be mounted north-south orientation for best summer operation, corresponding to solar cooling applications.

The following data shall be recorded during the test:

(1) Collector inlet and outlet temperatures.
(2) Total and diffused solar radiation on tracking plane.
(3) Liquid flow rate through collector.
(4) Heat exchanger inlet and outlet temperatures.
(5) Heat exchanger cooling fluid flow rate.
(6) Ambient temperature.
(7) Collector tracking angle.

The thermal performance evaluation data shall be obtained at inlet temperatures of approximately 140°, 190°, 220°, and 270°F at 10 GPM.

6.3.2 Procedure

1. Bring the collector out of stow and switch it to automatic tracking mode.

2. Initiate operation of the data acquisition system to record data and check to verify all necessary channels are operational.

3. Adjust the fluid flow rate to 10 GPM.

4. Adjust the inlet temperature to the desired setting.

5. Maintain the reservoir temperature to approximately the collector inlet temperature by adjusting the heat exchanger cooling water flow rate.

6. Record all data continuously at two minute intervals at quasi-steady state conditions.

7. Record collector tracking angle at 30 minute intervals during the test.

6.0 TEST REQUIREMENTS AND PROCEDURES (Continued)

6.3.3 Test Results

The results obtained during these tests are shown in Figures 4 and 5. Figure 4 shows the thermal efficiency of all test data plotted with the direct solar radiation as parameter at fluid flow rate of 10 GPM. Figure 5 shows the thermal efficiency of all test data plotted with the total solar radiation as parameter at fluid flow rate of 10 GPM. Figure 7 depicts the thermal efficiency data fluid flow rate of 5 GPM.

All these figures show the scattering of test data. The source of the scattering will be analyzed in the following sections. Table III is the listing of data recorded during one of the efficiency tests.

6.0 TEST REQUIREMENTS AND PROCEDURES (Continued)

6.4 Collector All Day Test

6.4.1 Test Requirement

Collector all day performance shall be conducted to determine the total amount of energy that can be delivered. The following data shall be recorded during the test:

(1) Collector inlet and outlet temperature.
(2) Total and diffused solar radiation on tracking plane.
(3) Liquid flow rate through collector.
(4) Heat exchanger inlet and outlet temperature.
(5) Heat exchanger cooling fluid flow rate.
(6) Ambient temperature.
(7) Collector tracking angle.

The all day thermal performance evaluation data shall be obtained at inlet temperatures of 140°F, 190°F, 220°F, and 270°F at 10 GPM.

6.4.2 Procedures

1. Bring the collector out of stow and switch it to automatic tracking mode.

2. Initiate operation of the data acquisition system to record data and check to verify all necessary channels are operational.

3. Adjust the fluid flow rate to 10 GPM.

4. Adjust the inlet temperature to the desired setting.

5. Maintain the reservoir temperature to approximately collector inlet temperature by adjusting the heat exchanger cooling water flow rate.

6. Record all data continuously at two minute intervals at quasi-steady state conditions.

7. Record collector tracking angle at 30 minute intervals during the test.

6.4.3 Test Results

The results of the all day test are shown in Figure 8. Table IV is the listing of data recorded during one of the all day tests. It is also important to know how this collector performs during an intermittent day because not every day of the year is a clear day. Figure 16 and 17 show the relation between the solar radiation and the collector thermal performance during a clear day and an intermittent day respectively.

6.0 **TEST REQUIREMENTS AND PROCEDURES** (Continued)

6.5 **Collector Heat Loss Test**

6.5.1 **Test Requirement**

A collector heat loss test shall be conducted to determine the heat loss coefficient. The collector shall be in the stow position, with the reflector surface and receiver tube covered so that no reflected solar radiation will be intercepted by the collector. The following data shall be recorded during the test:

(1) Collector inlet and outlet temperature.
(2) Collector flow rate.
(3) Ambient temperature.

6.5.2 **Procedures**

1. Cover the reflector surface and receiver tube.

2. Adjust the fluid flow rate.

3. Adjust the inlet temperature to the desired setting by using the inline heaters in the fluid loop.

4. Record all data continuously at two minute intervals at quasi-steady state conditions.

6.5.3 **Results**

The results of this test are presented in Figure 12.

7.0 ANALYSIS

7.1 Time Constant Test

Two methods are proposed by ASHRAE 93-77 for conducting a time constant test; however, due to facility limitation, neither one is applied. The method used here was abruptly reducing the solar flux to zero by turning the collector back to stow position and maintaining a constant flow rate and inlet temperature while obtaining data.

According to the definition of time constant given in ASHRAE 93-77, it is the time required for the ratio of the differential temperature at time t to the initial differential temperature to reach .368, when solar radiation is reduced to zero. It can be expressed as:

$$\frac{T_{f,e,t} - T_{f,i}}{T_{f,e,ini} - T_{f,i}} = .368 \qquad (1)$$

If the inlet fluid temperature cannot be controlled to within 2° of ambient air temperature, then the following equation must be used:

$$\frac{U_L(T_{f,i} - T_a) + \frac{\dot{m}C_p}{A_g}(T_{f,e,t} - T_{f,i})}{U_L(T_{f,i} - T_a) + \frac{\dot{m}C_p}{A_g}(T_{f,e,ini} - T_{f,i})} = .368 \qquad (2)$$

where:

$T_{f,e,t}$	Outlet fluid temperature at time t
$T_{f,i}$	Inlet fluid temperature
$T_{f,e,ini}$	Initial outlet fluid temperature
$\dot{m}$	Fluid mass flow rate
C_p	Specific heat of fluid
A_g	Collector gross area
U_L	Collector heat loss coefficieny, determined from the slope of the efficiency curve
T_a	Ambient temperature

The inlet fluid was not maintained within ±2°F of the ambient, hence equation (2) was used for evaluation.

7.0 ANALYSIS (Continued)

7.1 Time Constant Test (Continued)

$$\frac{.115\ (147 - 65.5) + \dfrac{9.56 \times 60 \times 3.7}{560}\ (T_{f,e,t} - 147)}{.115\ (147 - 65.5) + \dfrac{9.56 \times 60 \times 3.7}{560}\ (178 - 147)} = .368$$

Therefore,

$$T_{f,e,t} = 156.8°F.$$

From Figure 2, the time constant was determined to be 58 seconds for the four collector array.

7.0 ANALYSIS (Continued)

7.2 Collector Tracking Accuracy

The Solar Kinetics line concentrating collector can be categorized as a cylindrical optical system. It will focus the beam radiation to the receiver tube if the focal axis, the vertex line of the reflector, and the sun lie in a plane. Thus, for this type of system, it is possible to rotate the collector in one axis to meet this requirement. This axis of rotation may be north-south, east-west, or inclined and parallel to the earth's axis. For all the tests conducted in this report, the collector is rotating about the north-south axis from the east in the morning to the west in the afternoon.

Figure 3 shows the effect of being off track on the collector efficiency. As much as a 10 percentage point drop of the efficiency will occur when the collector tracking is missed by only 1 degree. Therefore, tracking accuracy is critical to the operation of a concentrating collector. The accuracy of tracking can be determined by monitoring the collector rotation angle. The following equations govern the collector rotation angle:

The declination, d, can be found from the approximate equation of Copper (1969):

$$d = 23.45 \text{ SIN } \left(360 \frac{284 + n}{365}\right) \qquad (1)$$

where n is the Julian day of the year.

The local standard time is converted to solar time in order to determine the sun's hour angle,

$$\text{Solar time} = \text{Standard Time} + E + 4\,(L_{st} - L_{loc}) \qquad (2)$$

where:

E = Equation of time, in minutes.

L_{st} = Standard meridian of the local time zone.

L_{loc} = Longitude of the location in degree, west.

The solar altitude angle 'a' is determined as:

$$\sin(a) = \cos(L)\cos(d)\cos(h) + (\sin(L)\sin(d)$$

where:

L = Latitude

h = hour angle from solar noon

d = declination angle

a = altitude angle

7.2 Collector Tracking Accuracy (Continued)

The azimuth angle, b, from solar south is:

$$\sin(b) = \frac{\cos(d)\,\sin(h)}{\cos(a)}$$

The rotation angle of a north-south axis collector is a function of the solar altitude and azimuth angle. It is defined by the following relations for a line concentrating collector mounted on a north-south orientation:

$$r = \tan^{-1}\frac{\tan(a)}{\cos(b)}$$

where:

r = Rotation angle
b = Solar azimuth angle
a = Solar altitude angle

However, this equation cannot be applied at solar noon. The rotation angle is 90° at solar noon. Table V shows the hourly rotation angle at 21st day of each month. It indicates that the collector rotation speed is not constant. Table VI shows the collector rotation speed for each hour at 21st day of each month.

7.3 Thermal Performance Test

7.3.1 Collector Instantaneous Efficiency

$$Q_u = A_a I_b [\rho \gamma (\tau d)] - U_L A_r (T_{ave} - T_a) = \dot{m} C_p (T_{out} - T_{in}) \quad (1)$$

where:

Q_u	= useful energy gain
A_a	= collector aperture area
I_b	= direct beam solar radiation
ρ	= specular reflectance of the reflector surface
γ	= intercept factor, the fraction of specularly reflected radiation that is intercepted by reciever
$(\alpha\tau)$	= the transmittance absorption produce of receiver
U_L	= heat loss coefficient
A_r	= receiver area
T_{ave}	= average fluid temperature
T_a	= ambient temperature
$\dot{m}$	= mass flow rate
C_p	= specific heat of the heat transfer fluid

The efficiency of a collector is defined as the ratio of useful energy gain to the available energy. Therefore, the efficiency, η, can be expressed as:

$$\eta = \frac{Q_u}{IA_a} = \rho \gamma (\alpha\tau) - U_L \frac{A_r}{A_a} \left(\frac{T_{ave} - T_a}{I}\right) \quad (1)$$

In order to compare with the flat-plate collector performance, the efficiency based on total solar radiation measured on the collector tracking plane is also calculated. The thermal efficiency of the Solar Kinetics T-700 line concentrating collector determined from test data is given by the following equations:

$$\eta = .592 - .115 \left(\frac{T_{ave} - T_a}{I_{dir}}\right) \quad (2)$$

$$\eta = .437 - .0006 \left(\frac{T_{ave} - T_a}{I_{tot}}\right) \quad (3)$$

7.3.1 Collector Instantaneous Efficiency (Continued)

However, these efficiencies were calculated based on a four collector array.

Scattering of test data can be seen in Figures 4 and 5. However, the scattering of test data is more severe in Figure 5 than in Figure 4, where the parameter was based on the total solar radiation. Figure 5 shows that if the test data were grouped with ranges of diffused solar fractions, it is found that the thermal efficiency will decrease with the increase of the diffused solar fraction, when the efficiency is calculated based on total solar radiation.

But, this trend is not as pronounced when the efficiency is calculated based on the direct solar radiation. Since the direct beam radiation is smaller when the diffused fraction is higher and the efficiency of a collector is calculated based on a smaller direct beam radiation. Therefore, the intercept and slope derived from the efficiency calculation based on total solar radiation is meaningless if the diffused solar radiation fraction is not identified. Figure 6 shows clear separation of data when the diffused fractions are grouped in the ranges of 0.0 ~.15, .15 ~.25, and .25 ~.35. Insufficient data were obtained with the diffuse fraction higher than 30%, so the efficiency curve was extrapolated to indicate the effect. Theoretically, at 0% diffuse fraction, the two efficiency curves, based on direct and total solar radiation, should coincide.

The diffused fraction changes the intercept of the efficiency curve, however, the slope will not be changed. The diffused fraction only effects the collector's optical efficiency, not the heat losses. Therefore, parallel lines can be drawn through each group of the data points.

From Figure 6, the intercept and the slope for each of the efficiency curve are:

$$\eta_1 = .58 - .176\ P \qquad f_d = .10$$

$$\eta_2 = .49 - .176\ P \qquad f_d = .22$$

$$\eta_3 = .43 - .176\ P \qquad f_d = .33$$

where:

f_d indicates the diffused fraction.

The efficiency of a concentrating collector based on total solar radiation can be expressed as

$$\eta = (1 - f_d)\rho\gamma(\tau\alpha) - U_L \frac{A_r}{A_a}\left(\frac{T_{ave} - T_a}{I_{tot}}\right)$$

Therefore, equation (3) is no longer valid and should be replaced with the following equation:

$$\eta = .64\ (1 - f_d) - .176\left(\frac{T_{ave} - T_a}{I_{tot}}\right)$$

7.3.2 Collector All Day Efficiency

Figure 8 shows the results of the collector all day test. These data were obtained over several days, with the inlet temperature maintained constant during each of the test periods. The efficiency calculation was based on the direct solar radiation. For all tests, it shows that the efficiency of the tracking concentrator was almost constant at one inlet temperature with slightly lower values at noon, due to the maximum incident angle occurring at noon.

As shown in Table V, the incident angle for this collector during the test period is varied from 17 degrees at 8 o'clock solar time to 47 degrees at solar noon, in September and October.

7.3.3 Solar Radiation

Solar Radiation was measured using pyranometers mounted on the collector plane and tracking with the collector. One of the pyranometers measures the total solar radiation on the collector plane, and the other one with shadowing disk to block the direct solar radiation, measures the diffused solar radiation on the collector plane. Thus, the direct solar radiation on the collector plane will be the difference between total solar radiation and the diffused solar radiation. A separate normal incident pyrheliometer which measures the direct solar radiation was recorded. In order to compare the pyrheliometer measurement with the tracking plane measurement, a cosine correction will be applied to the value of the tracking plane measurement. Because the pyrheliometer is always normal to the sun, while the direct solar radiation always has an incident angle to the tracking collector.

$$I_{dir} = (I_{tot} - I_{dif})/\cos\Theta_i$$

where:

Θ_i = incident angle

7.0 ANALYSIS (Continued)

7.3 Thermal Performance Test (Continued)

7.3.3 Solar Radiation (Continued)

Table VII shows the direct solar radiation derived from the collector tracking plane measurements agree well with the pyrheliometer measurements. Figure 9 shows the solar radiation of a typical clear day. The shadowing disk was so adjusted that the direct beam is always blocked. Figure 10 shows the solar radiation measured from the tracking plane in which two of the three shadowing disks were not blocking the beam portion of the total solar radiation.

7.3.4 Return Line Losses

To determine the return line heat losses, two temperatures were monitored during the test. One at the collector outlet and the other one at the inlet to the heat exchanger. The return line is approximately 125 ft. of 1" stainless steel piping. It is insulated with 1½" thick glass-fiber pipe insulation wrapped with aluminum pipe covering for weather protection.

The energy balance for a steady state condition is:

$$Q_{loss} = \dot{m}C_p \left(T_{out} - T_{in_{HX}}\right) = h\,A\,\left(T_{out} - T_a\right) \qquad (1)$$

where:

Q_{loss}	= line losses
$\dot{m}$	= flow rate
C_p	= specific heat of hear transfer fluid
T_{out}	= collector outlet temperature
$T_{in_{HX}}$	= heat exchanger inlet temperature
h	= heat loss coefficient
A	= pipe surface area
T_a	= ambient temperature

Rearranging equation (1), one yields

$$\frac{T_{out} - T_{in_{HX}}}{T_{out} - T_a} = \left(\frac{hA}{\dot{m}C_p}\right) = \text{Constant} \qquad (2)$$

7.0 ANALYSIS (Continued)

7.3 Thermal Performance Test (Continued)

7.3.4 Return Line Losses (Continued)

Figure 11 is the plot of $(T_{out} - T_{in_{HX}})$ against $(T_{out} - T_a)$ at the flow rates under the test. Equation (2) indicated that a straight line can be drawn through each set of the data points.

The heat loss coefficient does not vary significantly with the flow rate when the flow inside the tube is fully developed turbulent flow. Therefore, the heat loss coefficient, (hA), can be determined as:

$$(hA) = (\dot{m}C_p)_1 \text{ Constant}_1 = (\dot{m}C_p)_2 \text{ Constant}_2$$

From Figure 11 the heat loss coefficients for the 5.5 GPM flow and 9.5 GPM are:

$$(hA)_1 = (\dot{m}C_p)_1 \text{ Constant}_1 = 3.7*5.5*60*2.76/200 = 16.84 \ ^{Btu}/_{hr°F}$$

$$(hA)_2 = (\dot{m}C_p)_2 \text{ Constant}_2 = 3.7*9.5*60*1.55/200 = 16.34 \ ^{Btu}/_{hr°F}$$

7.0 ANALYSIS (Continued)

7.4 Collector Heat Loss

The heat loss test is an alternate way of determining the slope (i.e. heat lost coefficient), of a collector efficiency curve. The energy balance for the heat loss is similar to the return line loss described above. It is described as:

$$Q_{loss} = \dot{m}C_p \, (T_{in} - T_{out}) = U_L A_r \, (T_{ave} - T_a) \qquad (1)$$

where:

Q_{loss} = Collector heat loss

$U_L A_r$ = Receiver tube heat loss

Rearranging equation (1),

$$\frac{T_{in} - T_{out}}{T_{in} - T_a} = \left(\frac{U_L A_r}{\dot{m}C_p}\right)$$

Figure 12 is the plot of $(T_{in} - T_{out})$ versus $(T_{ave} - T_a)$.

It indicates that a straight line cannot be drawn from the origin, instead, one can draw a straight line through the data points from $(T_{ave} - T_a)$ equal to 40. Therefore, the heat loss coefficient can be considered as a constant when the $(T_{ave} - T_a)$ is greater than 40°F.

$$\frac{T_{in} - T_{out}}{T_{ave} - T_a} = \left(\frac{U_L A_r}{\dot{m}C_p}\right) = .0243 \quad \text{for } (T_{ave} - T_a) \;\; 40°F$$

$$U_L A_r = \dot{m}C_p *.0243 - 9.7*3.7*.0243*60 = 52.33 \; Btu/hr°F$$

In the equation defining the efficiency for a concentrating collector, the heat loss coefficient is the negative of the slope which is:

$$\frac{U_L A_r}{A_a} = \frac{52.37}{560} = 0.093 \; \frac{Btu}{hr.\; ft.^2 \; °F}$$

and the efficiency equation becomes:

$$\eta = .592 - 0.093 \; \frac{T_{ave} - T_a}{I}$$

Although the ratio of heat loss coefficients determined from these two tests, $\frac{.115 - 0.093}{.115} = .19$, is large, their values are small. Figure 13 shows the efficiency curves obtained from the thermal efficiency test and from the heat loss test, noting these two curves are very close to each other.

TIME HH:MM:SS	T_{in} °F	T_{out} °F	$T_{amb.}$ °F	Flow gpm
9:38:19	147.0	178.0	65.5	9.55
9:38:24	147.0	178.0	65.5	9.55
9:38:29	147.0	178.0	65.5	9.55
9:38:34	147.1	178.0	65.5	9.55
9:38:39	147.1	178.0	65.8	9.55
9:38:44	147.1	178.0	65.9	9.56
9:38:49	147.1	177.1	65.8	9.56
9:38:54	147.2	175.6	65.3	9.56
9:38:59	147.2	173.7	65.2	9.56
9:39:04	147.2	171.6	65.1	9.56
9:39:09	147.2	169.5	65.1	9.56
9:39:14	147.2	167.3	65.1	9.56
9:39:19	147.2	165.0	65.1	9.55
9:39:24	147.2	162.6	65.1	9.57
9:39:29	147.3	160.3	65.1	9.60
9:39:34	147.3	158.1	64.9	9.61
9:39:39	147.3	156.2	64.9	9.60
9:39:44	147.4	154.6	65.1	9.56
9:39:49	147.4	153.2	64.9	9.61

TABLE I. SOLAR KINETICS COLLECTOR TIME CONSTANT TEST RESULTS

SOLAR KINETICS TRACKING ACCURACY TEST 10-15-80

TIME	IN	OUT	DT	TAMB	GPM	DIR	DIF	TOT	D/T	QCOLL	INC	EFF	P
1000	140.0	141.4	1.4	68.0	9.7	200.9	33.2	234.2	0.14	2963	39.0	0.02	0.36
1001	138.9	140.9	2.0	68.6	9.7	200.8	33.2	233.9	0.14	4233	39.1	0.04	0.36
1002	138.5	139.9	1.4	68.6	9.7	201.1	32.9	234.1	0.14	2968	39.1	0.03	0.35
1003	138.1	139.6	1.5	69.7	9.7	201.4	32.3	233.7	0.14	3186	39.2	0.03	0.34
1003	138.1	139.6	1.5	69.7	9.7	201.4	32.3	233.7	0.14	3186	39.2	0.03	0.34
1004	137.8	140.1	2.3	70.3	9.7	201.0	32.1	233.2	0.14	4908	39.3	0.04	0.34
1005	137.4	141.0	3.6	70.1	9.7	200.8	32.0	232.8	0.14	7630	39.4	0.07	0.34
1006	137.2	143.8	6.6	70.0	9.7	200.7	31.9	222.7	0.14	14001	39.5	0.12	0.35
1007	137.5	149.7	12.2	70.5	9.7	200.8	31.8	232.7	0.14	25970	39.6	0.23	0.36
1008	138.4	157.8	19.4	70.6	9.7	200.7	32.1	232.8	0.14	41223	39.7	0.37	0.39
1009	140.2	164.9	24.7	70.1	9.7	201.0	32.1	233.1	0.14	52569	39.8	0.47	0.41
1010	140.3	169.4	29.1	70.4	9.7	201.3	31.8	233.0	0.14	61932	39.9	0.55	0.42
1011	142.7	170.5	27.8	70.0	9.7	201.0	31.7	232.7	0.14	58627	39.9	0.52	0.43
1012	145.1	172.1	27.0	70.3	9.6	201.7	31.7	233.0	0.14	59051	40.0	0.52	0.44
1013	146.1	175.5	29.4	70.7	9.6	201.0	31.6	232.5	0.14	[illegible]	40.1	0.55	0.45
1014	147.3	176.3	29.0	70.4	9.6	201.8	31.6	233.5	0.14	61021	40.2	0.54	0.45
1015	148.6	176.4	27.8	70.3	9.6	201.5	31.5	233.1	0.14	58129	40.3	0.52	0.46
1016	149.2	175.7	26.5	69.3	9.5	201.4	31.5	233.0	0.14	55476	40.3	0.49	0.46
1017	148.8	173.1	24.3	69.2	9.5	201.2	31.6	232.8	0.14	52098	40.4	0.45	0.45
1018	148.8	167.2	18.4	70.2	9.6	201.0	31.7	232.7	0.14	38614	40.5	0.34	0.44
1019	151.0	162.1	11.1	70.5	9.5	201.4	31.8	233.2	0.14	[illegible]	40.6	0.21	0.43
1020	151.1	159.1	8.0	69.3	9.5	201.7	31.8	233.5	0.14	16747	40.7	0.15	0.42
1021	150.6	155.8	5.2	69.6	9.5	202.0	31.9	233.9	0.14	10672	40.7	0.10	0.41
1022	149.4	153.3	3.9	70.5	9.5	201.6	31.9	233.5	0.14	8142	40.8	0.07	0.40
1023	149.3	152.9	2.6	70.7	9.5	201.2	32.1	233.4	0.14	5407	40.9	0.05	0.39
1024	146.1	148.3	2.2	71.1	9.6	200.7	32.4	233.1	0.14	5717	41.0	0.06	0.38
1025	147.0	147.3	0.3	71.6	9.6	200.4	32.6	233.0	0.14	570	41.0	0.01	0.33
1026	146.3	147.7	1.4	72.6	9.6	200.3	32.7	233.0	0.14	2950	41.1	0.03	0.37
1027	145.2	147.3	2.1	72.7	9.6	199.7	32.6	232.4	0.14	4429	41.2	0.04	0.37
1028	144.3	146.2	1.9	71.5	9.6	199.5	32.7	232.2	0.14	4012	41.3	0.04	0.37
1029	143.8	145.2	1.4	71.4	9.6	199.0	32.8	231.9	0.14	2957	41.3	0.03	0.37
1030	143.3	144.6	1.3	71.5	9.6	198.5	32.9	231.4	0.14	2748	41.4	0.02	0.36

IN: Collector Inlet

OUT: Collector Inlet

DT: Outlet-Inlet

TAMB: Ambient Temp.

GPM: Flow Rate

DIR: Direct Solar

DIF: Diffused Solar

TOT: Total Solar

D/T: Dif/Tot

QCOLL: Energy Collected

INC: Incident Angle

EFF: Efficiency

P: $(T_{ave} - T_a)/DIR$

TABLE II. SOLAR KINETICS COLLECTOR TRACKING ACCURACY TEST RESULTS

SOLAR KINETICS 10-06-80

TIME	IN	OUT	DT	TAMB	GPM	DIR	DIF	TOT	D/T	QCOLL	INC	EFF	P
905	134.9	169.8	34.9	53.2	9.9	238.2	32.7	271.0	0.12	75734.	30.3	0.57	0.42
915	139.9	175.2	35.3	53.0	9.7	236.6	33.0	269.6	0.12	75390.	31.4	0.57	0.44
925	141.8	177.5	35.7	54.1	9.9	243.1	28.6	271.7	0.11	77390.	32.4	0.57	0.43
935	142.8	177.9	35.1	55.2	9.9	238.7	27.0	265.7	0.10	76336.	33.5	0.57	0.44
945	142.8	178.1	35.3	55.7	10.0	239.9	27.2	267.0	0.10	76981.	34.4	0.57	0.44
955	142.6	177.5	34.9	55.1	9.9	237.8	26.7	264.5	0.10	75636.	35.4	0.57	0.44
1005	141.9	176.4	34.5	55.6	9.9	236.6	26.3	262.9	0.10	75154.	36.2	0.57	0.44
1015	141.3	175.5	34.2	55.8	9.9	233.9	26.0	259.8	0.10	74299.	37.0	0.57	0.44
1025	140.8	174.9	34.1	56.0	10.0	221.7	25.5	257.2	0.10	74438.	37.8	0.57	0.44
1035	140.2	174.3	34.1	58.6	10.0	231.7	25.2	256.9	0.10	74400.	38.5	0.57	0.43
1045	139.8	173.3	33.5	57.6	9.9	227.8	24.9	252.7	0.10	72595.	39.1	0.57	0.43
1055	139.4	172.8	33.4	58.1	9.9	227.1	25.0	252.2	0.10	72253.	39.6	0.57	0.43
1105	138.8	171.7	32.9	59.5	10.0	225.2	24.4	249.6	0.10	71927.	40.1	0.57	0.43
1115	138.2	171.1	32.9	59.6	10.0	224.5	24.2	248.7	0.10	72125.	40.5	0.57	0.42
1125	138.0	170.9	32.9	61.1	10.0	224.0	24.0	248.0	0.10	72135.	40.8	0.58	0.42
1145	132.9	164.9	32.0	60.5	10.0	220.1	24.1	244.2	0.10	69973.	41.2	0.57	0.40
1155	135.4	167.8	32.4	63.0	10.0	221.9	22.8	245.7	0.10	70052.	41.3	0.57	0.40
1215	172.5	204.6	32.1	63.1	9.7	222.8	24.3	249.1	0.10	68296.	41.2	0.54	0.56
1225	170.3	202.1	31.8	62.4	9.7	224.8	24.2	249.0	0.10	68866.	41.1	0.54	0.55
1235	170.7	202.6	31.9	63.2	9.6	224.8	24.0	248.9	0.10	67525.	40.8	0.54	0.55
1245	171.0	203.1	32.1	63.4	9.5	226.7	24.2	250.9	0.10	67154.	40.5	0.53	0.55
1255	171.3	203.8	32.5	64.0	9.5	228.0	24.6	252.6	0.10	66296.	40.1	0.53	0.54
1305	171.5	204.0	32.5	65.5	9.7	228.9	24.7	252.6	0.10	69594.	39.6	0.54	0.53
1315	171.8	205.0	33.2	65.0	9.6	232.0	25.0	257.0	0.10	70640.	39.0	0.54	0.53
1325	171.0	204.2	33.2	65.6	9.5	232.7	25.3	258.0	0.10	69595.	38.4	0.53	0.52
1335	169.9	203.2	33.3	66.2	9.7	234.0	25.2	259.2	0.10	71212.	37.7	0.54	0.51
1345	172.5	206.0	33.5	67.0	9.6	235.8	25.4	261.1	0.10	70496.	37.0	0.53	0.52
1355	172.3	206.4	34.1	67.1	9.3	236.1	25.8	261.9	0.10	70129.	36.1	0.53	0.52
1405	172.6	207.3	34.7	66.9	9.4	238.7	25.9	264.6	0.10	71969.	35.3	0.54	0.52
1415	171.8	207.2	35.4	67.9	9.6	241.3	26.0	267.3	0.10	75156.	34.3	0.56	0.50
1425	171.6	207.1	35.5	68.2	9.6	242.5	26.5	269.1	0.10	75059.	33.4	0.55	0.50
1435	171.8	207.3	35.5	67.0	9.6	242.4	26.9	270.3	0.10	75022.	32.3	0.55	0.50
1445	172.1	207.6	35.5	67.3	9.6	241.4	27.1	268.5	0.10	74579.	31.3	0.55	0.51
1455	171.8	207.5	35.7	68.0	9.6	242.6	27.1	269.8	0.10	75250.	30.1	0.55	0.50
1505	171.8	207.7	35.9	68.1	9.6	243.5	26.9	270.5	0.10	75545.	29.0	0.56	0.50

TABLE III. SOLAR KINETICS COLLECTOR ARRAY THERMAL EFFICIENCY TEST RESULTS

SOLAR KINETICS 10-?7-80

TIME	IN	OUT	DT	TAMB	GPM	DIR	DIF	TOT	D/T	QCOLL	INC	EFF	P
815	221.7	253.4	31.7	51.2	9.0	217.7	27.3	245.0	0.11	62975.	24.6	0.52	0.86
825	221.8	253.6	31.8	51.7	9.2	220.3	27.4	247.7	0.11	64699.	25.9	0.52	0.84
835	217.9	251.2	33.3	52.8	9.2	223.7	28.8	252.5	0.11	67736.	27.1	0.54	0.81
845	219.9	252.9	33.0	54.6	9.3	224.5	29.0	253.5	0.11	67956.	28.3	0.54	0.81
855	220.4	253.6	33.2	55.7	9.3	226.0	28.4	254.4	0.11	68444.	29.5	0.54	0.80
905	220.1	253.2	33.1	57.7	9.3	225.5	28.5	254.1	0.11	68212.	30.6	0.54	0.79
915	220.5	253.4	32.9	57.4	9.2	225.0	28.6	253.6	0.11	67333.	31.8	0.53	0.80
925	220.5	253.7	33.2	59.1	9.3	225.2	28.1	253.3	0.11	68232.	32.8	0.54	0.79
935	220.2	252.9	32.7	59.0	9.3	224.4	27.8	252.2	0.11	67373.	33.9	0.54	0.79
945	220.5	253.5	33.0	61.0	9.3	223.8	27.2	251.1	0.11	67726.	34.8	0.54	0.79
955	220.1	252.6	32.5	62.0	9.2	222.0	27.7	250.7	0.11	66549.	35.8	0.53	0.78
1005	219.6	251.9	32.3	63.7	9.3	222.3	27.3	249.6	0.11	66228.	36.6	0.53	0.77
1015	221.5	254.0	32.5	65.1	9.1	225.2	26.3	251.5	0.10	65769.	37.4	0.52	0.77
1025	219.7	251.6	31.9	64.8	9.3	220.6	25.0	245.5	0.10	65623.	38.2	0.53	0.77
1035	220.6	252.3	31.7	65.1	9.1	220.0	24.8	244.8	0.10	64840.	38.9	0.52	0.78
1045	220.7	252.3	31.6	64.9	9.3	218.2	24.3	242.4	0.10	64951.	39.5	0.53	0.79
1055	220.5	251.8	31.3	65.2	9.3	217.4	23.1	240.4	0.10	64290.	40.0	0.53	0.79
1105	221.3	252.2	30.9	67.2	9.2	216.3	22.4	238.7	0.09	63115.	40.5	0.52	0.78
1115	222.2	253.0	30.8	68.0	9.3	214.5	21.9	236.4	0.09	63534.	40.9	0.53	0.79
1135	218.8	249.5	30.7	69.4	9.2	213.7	21.9	235.6	0.09	62542.	41.5	0.52	0.77
1145	220.4	250.1	29.7	69.9	9.2	212.4	22.0	235.4	0.09	60581.	41.6	0.51	0.77
1155	219.9	250.3	30.4	70.1	9.2	212.0	21.9	234.9	0.09	61894.	41.7	0.52	0.77
1205	240.0	267.4	27.4	71.5	9.2	213.1	21.6	234.7	0.09	55725.	41.7	0.47	0.86
1215	255.0	282.4	27.4	70.7	9.0	212.1	22.6	235.7	0.10	55817.	41.6	0.46	0.93
1225	258.0	286.5	28.5	71.9	9.0	213.2	22.4	235.6	0.10	57225.	41.4	0.46	0.94
1235	266.6	294.4	27.8	72.3	8.8	213.5	22.8	236.3	0.10	54726.	41.2	0.46	0.98
1245	270.7	299.5	28.8	72.1	8.6	212.0	[illegible]	226.7	0.10	55227.	40.8	0.46	1.00
1255	270.4	298.3	27.9	71.9	8.8	211.9	25.3	237.2	0.11	54562.	40.4	0.46	1.00
1305	270.2	298.1	27.9	72.7	8.8	213.1	25.9	239.0	0.11	54484.	40.0	0.46	0.99
1315	271.2	300.2	29.0	72.2	8.7	215.4	26.5	242.0	0.11	55395.	39.4	0.46	0.99
1325	269.2	298.2	29.0	73.4	8.7	216.4	27.3	243.7	0.11	56028.	38.8	0.46	0.97
1335	271.8	301.0	29.2	73.0	8.5	213.4	27.8	246.2	0.11	55551.	38.1	0.45	0.98
1345	270.2	300.0	29.8	74.9	8.5	218.3	28.6	246.9	0.12	57537.	37.3	0.46	0.96
1355	270.0	300.2	30.2	75.8	8.4	218.8	28.9	247.7	0.12	56564.	36.5	0.46	0.96
1405	270.1	301.2	31.1	75.8	8.4	219.3	29.4	248.7	0.12	58229.	35.6	0.47	0.96
1415	270.7	302.1	31.4	75.1	8.4	219.2	29.5	248.7	0.12	58905.	34.7	0.46	0.96
1425	271.3	302.7	31.4	76.9	8.3	219.4	30.0	249.4	0.12	58267.	33.7	0.47	0.96
1435	269.4	301.3	31.9	76.4	8.3	219.3	30.6	249.9	0.12	59074.	32.6	0.48	0.95
1445	268.6	299.7	31.1	75.6	8.4	219.3	30.8	250.1	0.12	57879.	31.6	0.47	0.95
1455	270.9	303.4	32.5	75.5	8.2	219.5	30.5	250.0	0.12	59603.	30.4	0.48	0.96

TABLE III. SOLAR KINETICS COLLECTOR ARRAY THERMAL EFFICIENCY TEST RESULTS (Continued)

SOLAR KINETICS COLLECTOR ALL DAY TEST 10-09-80

TIME	IN	OUT	DT	TAMB	GPM	DIR	DIF	TOT	D/T	QCOLL	INC	EFF	P
830	145.7	199.1	53.4	65.3	5.1	192.7	34.0	227.6	0.15	59931.	27.1	0.56	0.56
840	147.1	201.4	54.3	66.7	5.2	195.2	35.7	230.8	0.15	62190.	28.3	0.57	0.55
850	147.7	202.7	55.0	68.2	5.2	198.3	36.6	234.8	0.16	62225.	29.5	0.56	0.54
900	147.8	203.3	55.5	69.7	5.2	200.2	37.0	237.2	0.16	63496.	30.7	0.57	0.53
910	147.8	202.7	54.9	69.9	5.3	198.9	37.8	236.7	0.16	63268.	31.9	0.57	0.53
920	147.6	202.4	54.8	70.7	5.2	199.4	38.8	238.2	0.16	62672.	33.0	0.56	0.52
930	147.2	202.0	54.8	72.1	5.2	198.6	39.3	237.8	0.17	63810.	34.0	0.57	0.52
940	147.2	201.9	54.7	73.2	5.3	199.1	39.2	238.4	0.16	63204.	35.0	0.57	0.51
950	147.2	201.9	54.7	74.1	5.2	200.1	39.0	239.1	0.16	62553.	36.0	0.56	0.50
1000	146.9	201.0	54.1	74.1	5.2	198.8	38.6	237.4	0.16	62186.	36.9	0.56	0.50
1010	146.7	200.6	53.9	75.5	5.3	198.1	38.3	236.4	0.16	62206.	37.7	0.56	0.50
1020	146.7	200.2	53.5	76.2	5.2	197.3	37.6	234.9	0.16	61546.	38.5	0.56	0.49
1030	146.9	199.8	52.9	76.4	5.2	196.6	36.6	233.1	0.16	60683.	39.3	0.55	0.49
1040	146.9	199.5	52.6	77.9	5.3	194.7	35.4	230.1	0.15	60600.	39.9	0.56	0.49
1050	146.8	199.6	52.8	78.1	5.2	195.1	34.3	229.4	0.15	60788.	40.5	0.56	0.49
1100	146.7	199.4	52.7	78.7	5.2	195.1	33.3	228.4	0.15	60472	41.0	0.55	0.48
1110	146.5	199.2	52.7	79.4	5.3	195.1	32.8	227.9	0.14	60912	41.5	0.56	0.48
1120	146.5	198.6	52.1	79.5	5.2	192.9	32.3	225.2	0.14	59663.	41.8	0.55	0.48
1130	146.3	198.1	51.8	80.1	5.3	192.6	32.4	225.0	0.14	59809.	42.1	0.55	0.48
1140	146.1	197.5	51.4	81.2	5.3	192.1	31.9	224.0	0.14	59395.	42.3	0.55	0.47
1150	145.8	196.9	51.1	79.5	5.3	192.1	31.5	223.6	0.14	59125.	42.4	0.55	0.48
1240	168.0	220.8	52.8	81.5	5.1	199.2	30.5	229.6	0.13	58994.	41.8	0.53	0.57
1250	168.7	221.2	52.5	83.0	5.1	201.3	30.4	231.7	0.13	59421.	41.4	0.53	0.56
1300	169.7	221.8	52.1	84.2	5.1	200.0	30.6	230.6	0.13	58644.	41.0	0.53	0.56
1310	170.1	224.2	54.1	85.0	5.1	205.0	30.5	235.5	0.13	60810.	40.4	0.53	0.55
1320	171.0	225.5	54.5	84.2	5.1	206.8	30.1	236.9	0.13	60697.	39.8	0.52	0.55
1330	171.4	226.9	55.5	85.0	5.0	208.0	30.8	238.8	0.13	61129.	39.2	0.52	0.55
1340	171.0	227.9	56.9	85.1	5.0	211.1	31.1	242.2	0.13	62445.	38.4	0.53	0.54
1350	171.3	227.3	56.0	84.1	5.0	209.3	32.1	241.4	0.13	61674.	37.7	0.53	0.55
1400	171.6	229.3	57.7	85.9	5.0	212.0	31.9	242.9	0.13	62973.	36.8	0.53	0.54
1410	172.1	230.3	58.2	85.6	4.9	213.1	32.7	245.8	0.13	63335.	35.9	0.53	0.54
1420	169.6	224.9	55.3	85.2	5.1	211.9	33.5	245.4	0.14	62201.	34.9	0.52	0.53
1430	171.0	229.5	58.5	85.7	5.0	210.2	32.0	242.2	0.13	64391.	33.9	0.55	0.55
1440	169.4	226.1	56.7	85.5	5.2	206.8	32.6	239.4	0.14	64609.	32.8	0.56	0.54
1450	170.9	225.8	54.9	84.0	5.1	208.3	33.1	241.4	0.14	62104	31.7	0.53	0.55
1500	172.3	229.8	57.5	85.6	5.1	213.2	32.0	245.3	0.13	64367.	30.6	0.54	0.54

TABLE IV. SOLAR KINETICS COLLECTOR ARRAY ALL DAY TEST RESULTS

Solar Time		8/16	9/15	10/14	11/13	12	Declination
	inc.	33.4	41.4	48.3	53.1	54.9	
Jan.	rot.	13.1	27.7	45.1	66.1	90.0	-20.1
	alt.	10.9	20.4	28.2	33.3	35.1	
	inc.	26.1	33.7	40.1	44.4	46.0	
Feb.	rot.	19.0	33.5	50.1	69.2	90.0	-11.2
	alt.	17.0	27.3	35.9	41.9	44.0	
	inc.	16.6	23.8	29.6	33.4	34.8	
Mar.	rot.	25.4	39.4	54.9	71.9	90.0	-0.0
	alt.	24.3	35.5	45.4	52.5	55.2	
	inc.	6.3	13.0	18.2	21.6	22.8	
Apr.	rot.	31.5	44.8	59.0	74.2	90.0	11.9
	alt.	31.3	43.3	54.5	63.4	67.2	
	inc.	1.1	5.3	10.2	13.3	14.4	
May	rot.	35.7	48.3	61.6	75.6	90.0	20.3
	alt.	35.7	48.0	59.9	70.4	75.6	
	inc.	3.8	2.5	7.2	10.3	11.3	
Jun.	rot.	37.2	49.5	62.5	76.0	90.0	23.4
	alt.	37.1	49.4	61.6	72.7	78.7	
	inc.	1.0	5.4	10.3	13.4	14.5	
Jul.	rot.	35.6	48.2	61.5	75.5	90.0	20.2
	alt.	35.6	47.9	59.9	70.4	75.5	
	inc.	6.7	13.5	18.7	22.2	23.3	
Aug.	rot.	31.3	44.5	58.8	74.1	90.0	11.4
	alt.	31.0	43.0	54.1	63.0	66.7	
	inc.	17.1	24.3	30.2	34.0	35.4	
Sept.	rot.	25.1	39.1	54.7	71.8	90.0	-0.6
	alt.	23.9	35.1	44.9	52.0	54.6	
	inc.	26.8	34.5	40.9	45.3	46.9	
Oct.	rot.	18.4	33.0	49.7	68.9	90.0	-12.1
	alt.	16.4	26.7	35.2	41.0	43.1	
	inc.	33.8	41.8	48.7	53.6	55.4	
Nov.	rot.	12.8	27.4	44.8	65.9	90.0	-20.6
	alt.	10.6	20.0	27.7	32.8	34.6	
	inc.	36.0	44.2	51.2	56.3	58.2	
Dec.	rot.	10.7	25.3	42.9	64.7	90.0	-23.4
	alt.	8.6	17.8	25.2	30.1	31.8	

inc. : Incident Angle
rot. : Rotation Angle
alt. : Altitude Angle

TABLE V. COLLECTOR INCIDENT ANGLE, ROTATION ANGLE AND SUN'S ALTITUDE ANGLE ON THE 21st DAY OF EACH MONTH

Month \ Time	8-9	9-10	10-11	11-12
JAN	14.6	17.4	21.0	23.9
FEB	14.5	16.6	19.1	20.8
MAR	14.0	15.5	17.0	18.1
APR	13.3	14.2	15.2	15.8
MAY	12.6	13.3	14.0	14.4
JUNE	12.3	13.0	13.5	14.0
JULY	12.6	13.3	14.0	14.5
AUG	13.2	14.3	15.3	15.9
SEPT	14.0	15.6	17.1	18.2
OCT	14.6	16.7	19.2	21.1
NOV	14.6	17.4	21.1	24.1
DEC	14.6	17.6	21.8	25.3

TABLE VI. COLLECTOR ROTATION SPEED ON THE 21st DAY OF EACH MONTH IN DEGREES PER HOUR

	10/6/80			10/7/80		
Solar Time	Pyr.	SKI	Δ %	Pyr.	SKI	Δ %
9:00	850	872	-2.5	826	826	0.4
:15	874	874	0	838	836	0.2
:30	886	908	-2.4	850	848	0.2
:45	898	917	-2.1	850	862	-1.4
10:00	898	924	-2.8	886	869	2.0
:15	898	923	-2.7	886	880	0.7
:30	898	933	-3.8	898	887	1.2
:45	898	930	-3.4	862	894	-3.4
11:00	898	928	-3.2	862	895	-3.7
:15	898	931	-3.5	874	899	-2.8
:30	898	933	-3.8	874	897	-2.6
:45	910	922	-1.3	874	900	-2.9
12:00	910	931	2.3	874	899	-2.9
:15	910	938	-3.0	874	900	-2.9
:30	910	936	-2.8	850	896	-5.1
:45	898	940	-4.5	850	888	-4.3
13:00	898	937	-4.2	832	879	-5.3
:15	898	941	-4.6	826	879	-6.0
:30	898	932	-3.6	826	874	-5.5
:45	898	931	-3.5	820	867	-5.4
14:00	898	922	-2.6	820	855	-4.1
:15	898	921	-2.5	802	842	-4.8
:30	886	908	-2.4	778	827	-5.9
:45	874	891	-1 9			
15:00	862	878	1.8			

Pyr.: Pyrheliometer measurement
SKI: Tracking plane measurement = $(I_{tot} - I_{dif})/COS\theta_i$
Δ%= (Pyr-SKI)/SKI *100

TABLE VII . COMPARISON OF DIRECT SOLAR RADIATION DATA FROM PYRHELIOMETER WITH THE TRACKING PLANE MEASUREMENTS

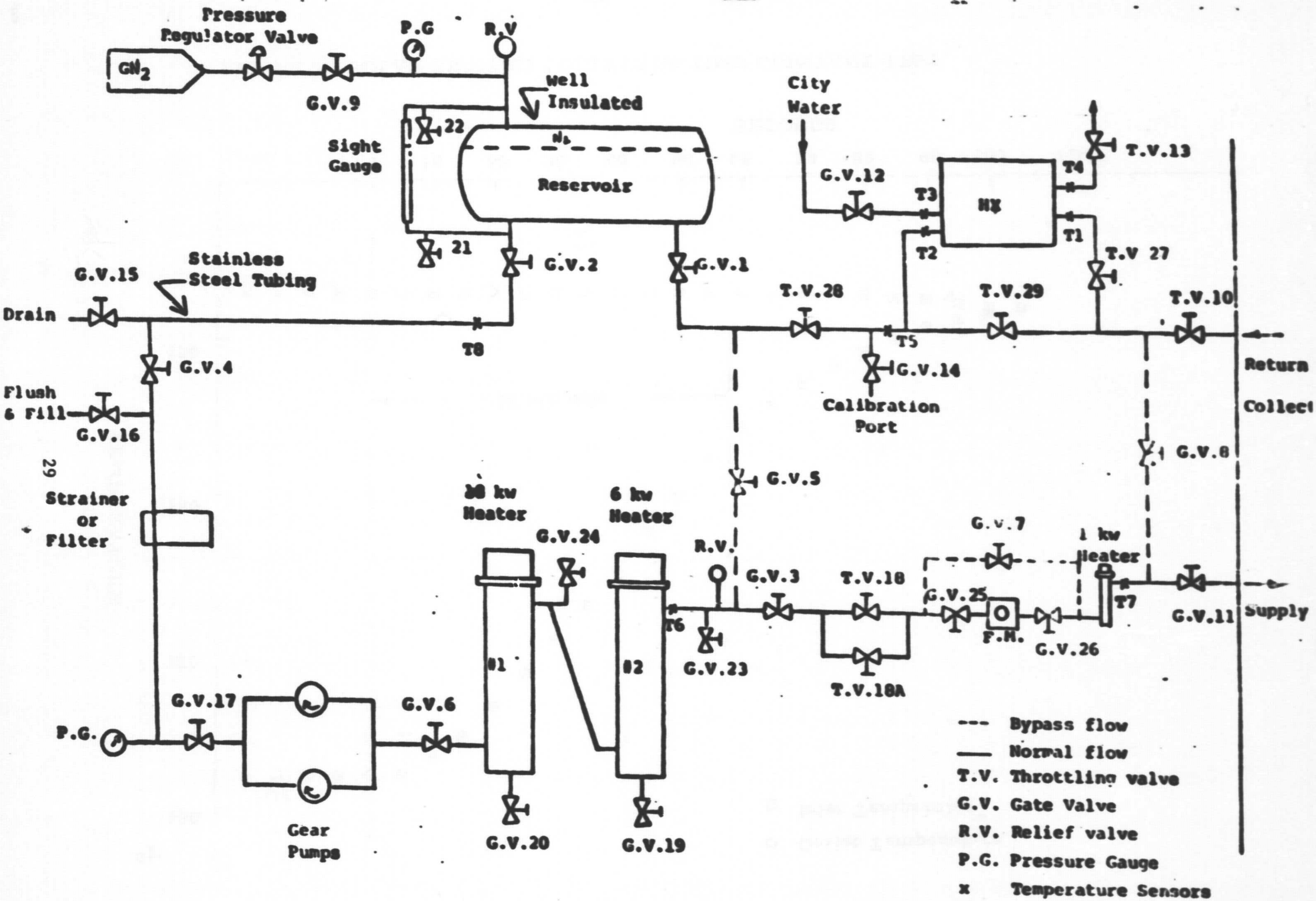

FIGURE 1. NASA HIGH TEMPERATURE FLUID SUPPLY LOOP

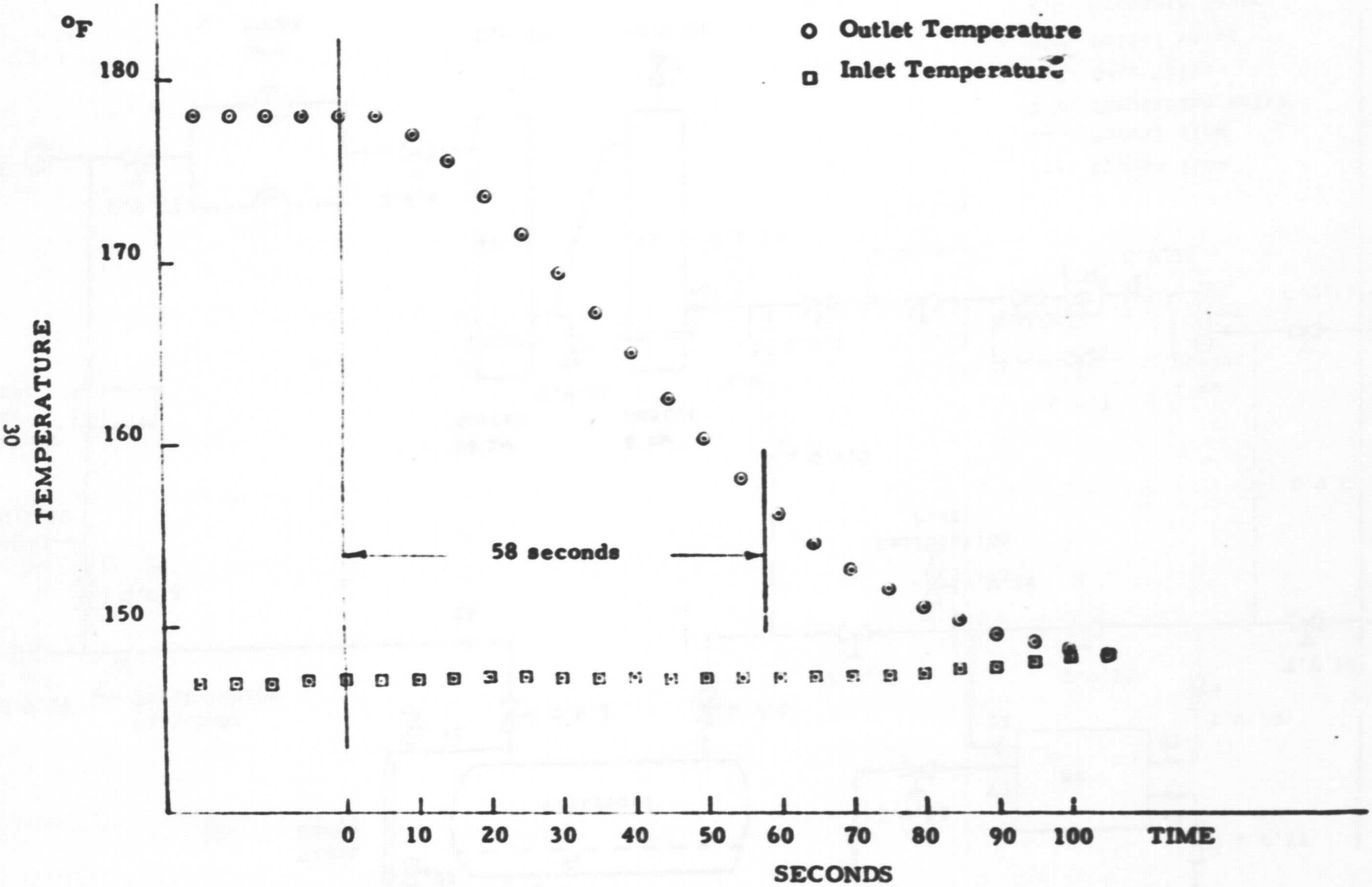

FIGURE 2. SOLAR KINETICS COLLECTOR TIME CONSTANT TEST

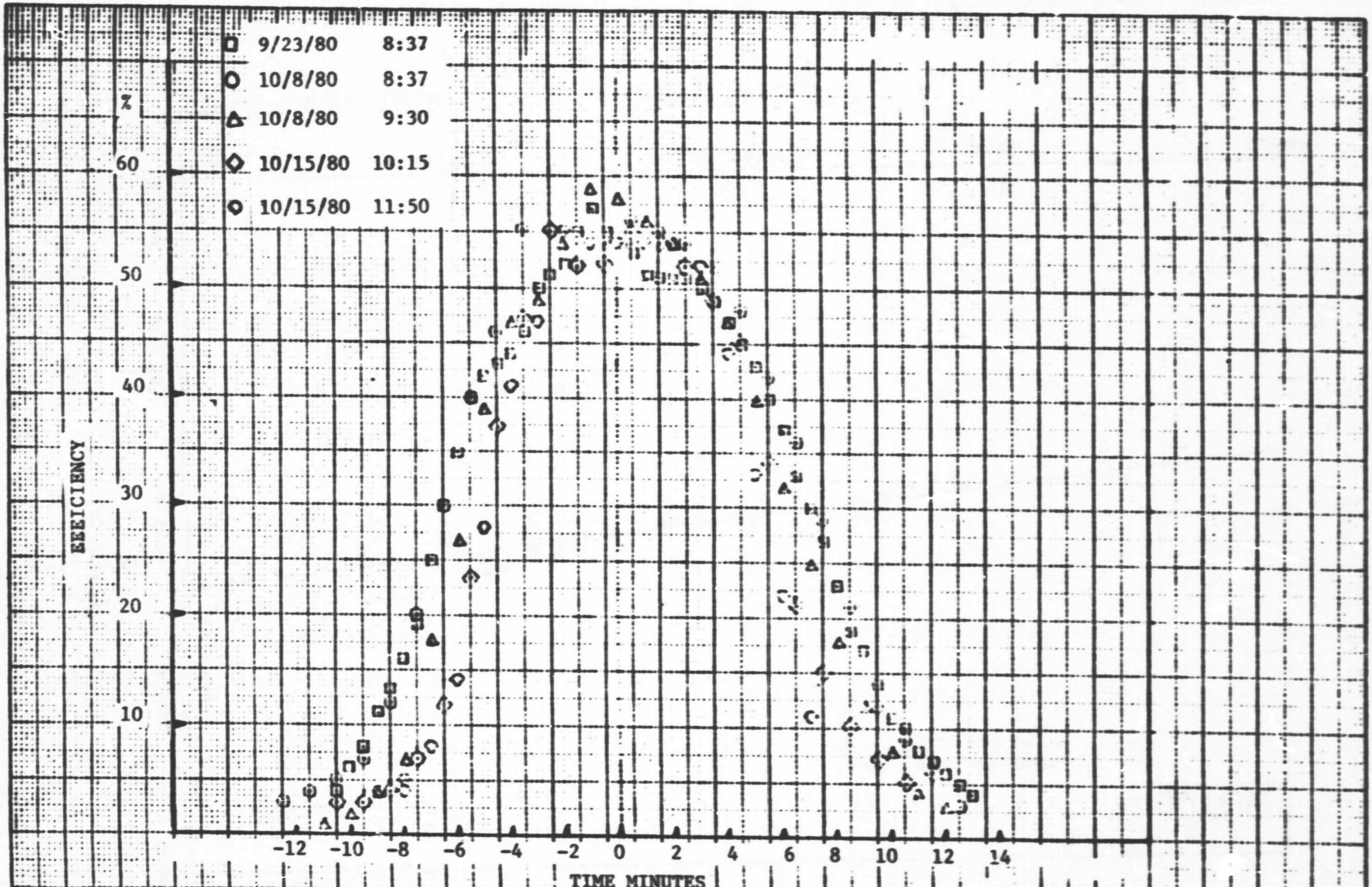

FIGURE 3. THE EFFECT OF COLLECTOR OFF TRACK TO ITS PERFORMANCE

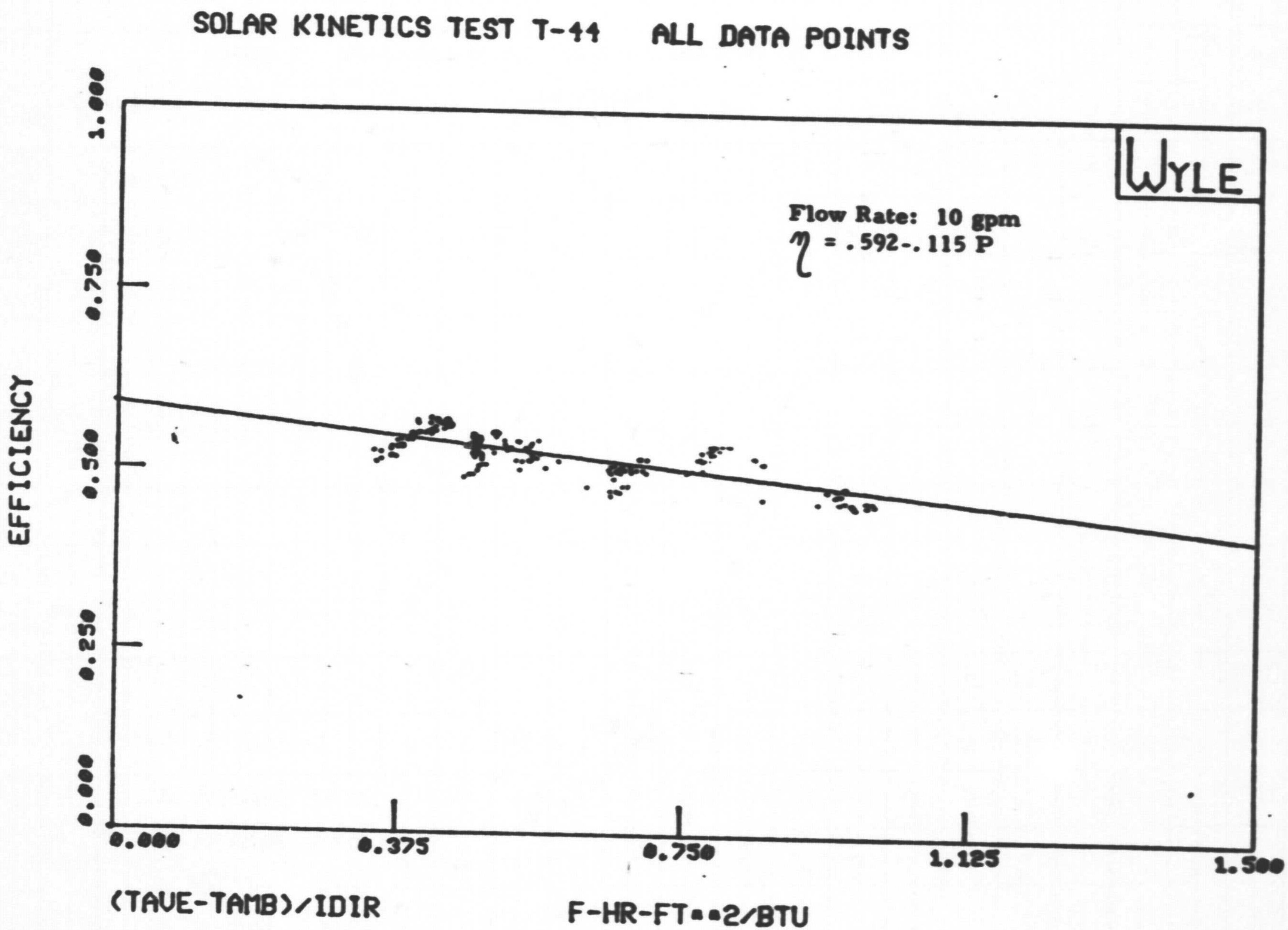

FIGURE 4. COLLECTOR THERMAL EFFICIENCY BASED ON DIRECT SOLAR RADIATION

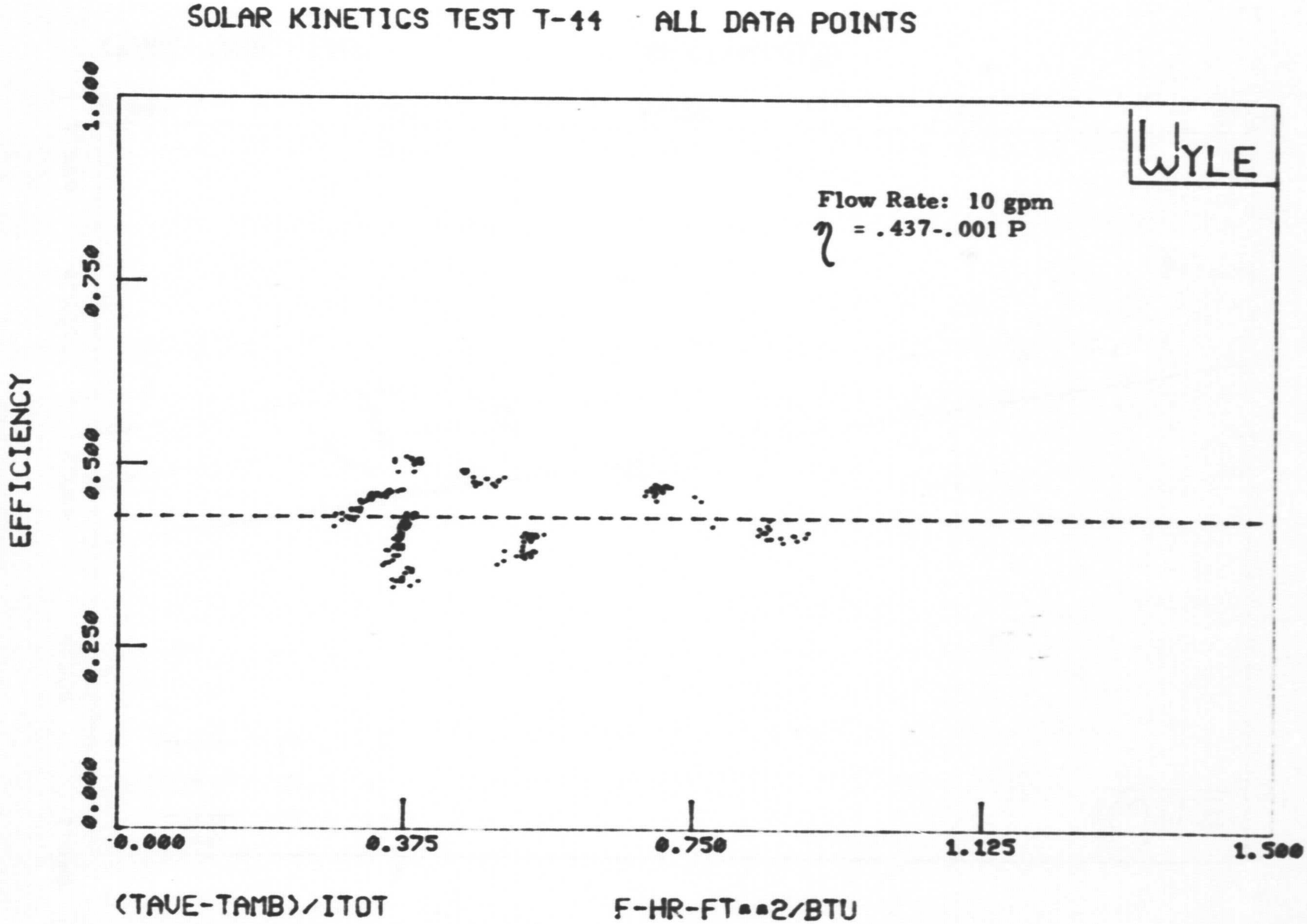

FIGURE 5. COLLECTOR THERMAL EFFICIENCY BASED ON TOTAL SOLAR RADIATION

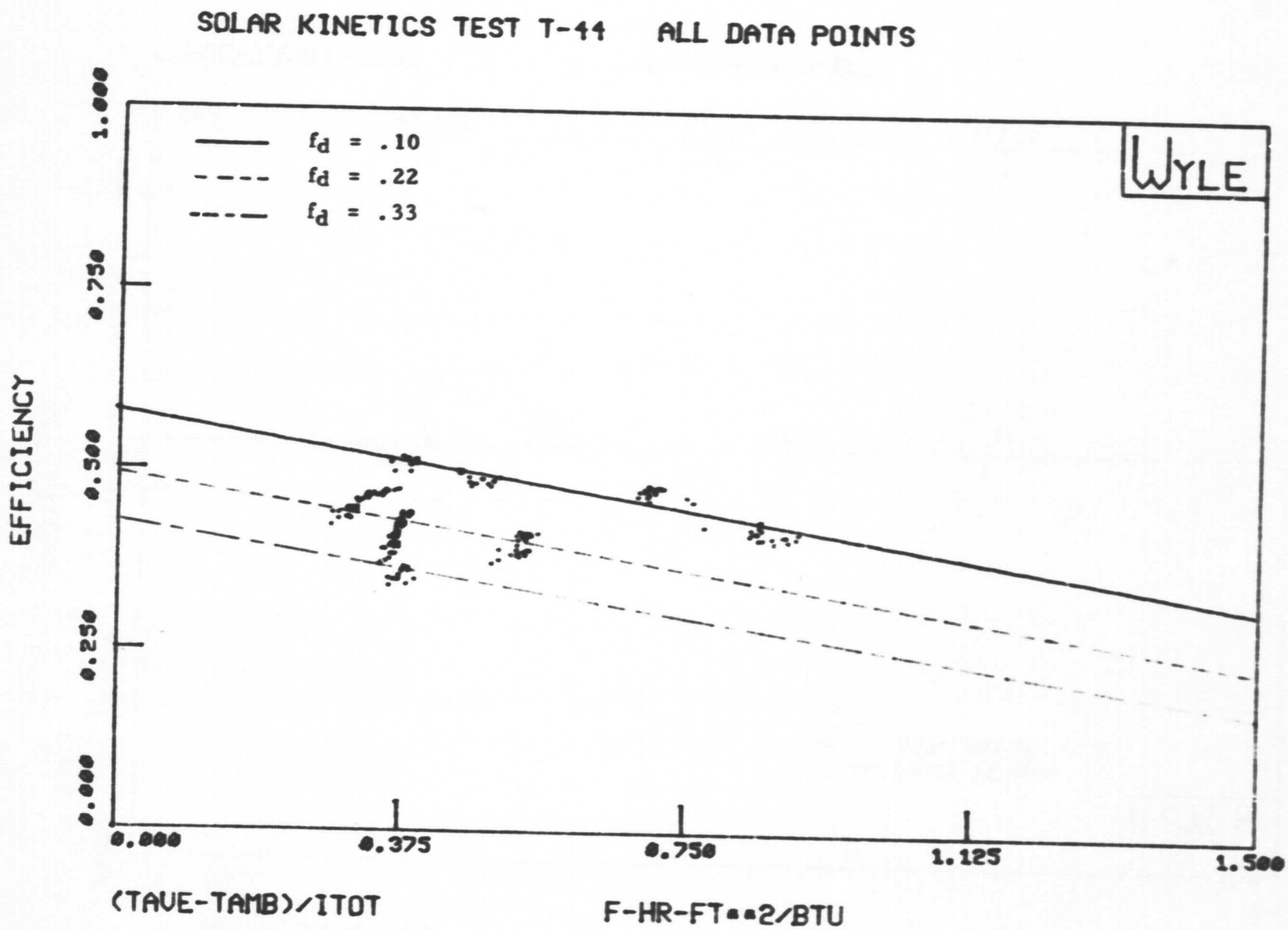

FIGURE 6. COLLECTOR THERMAL EFFICIENCY BY DIFFUSED SOLAR FRACTION

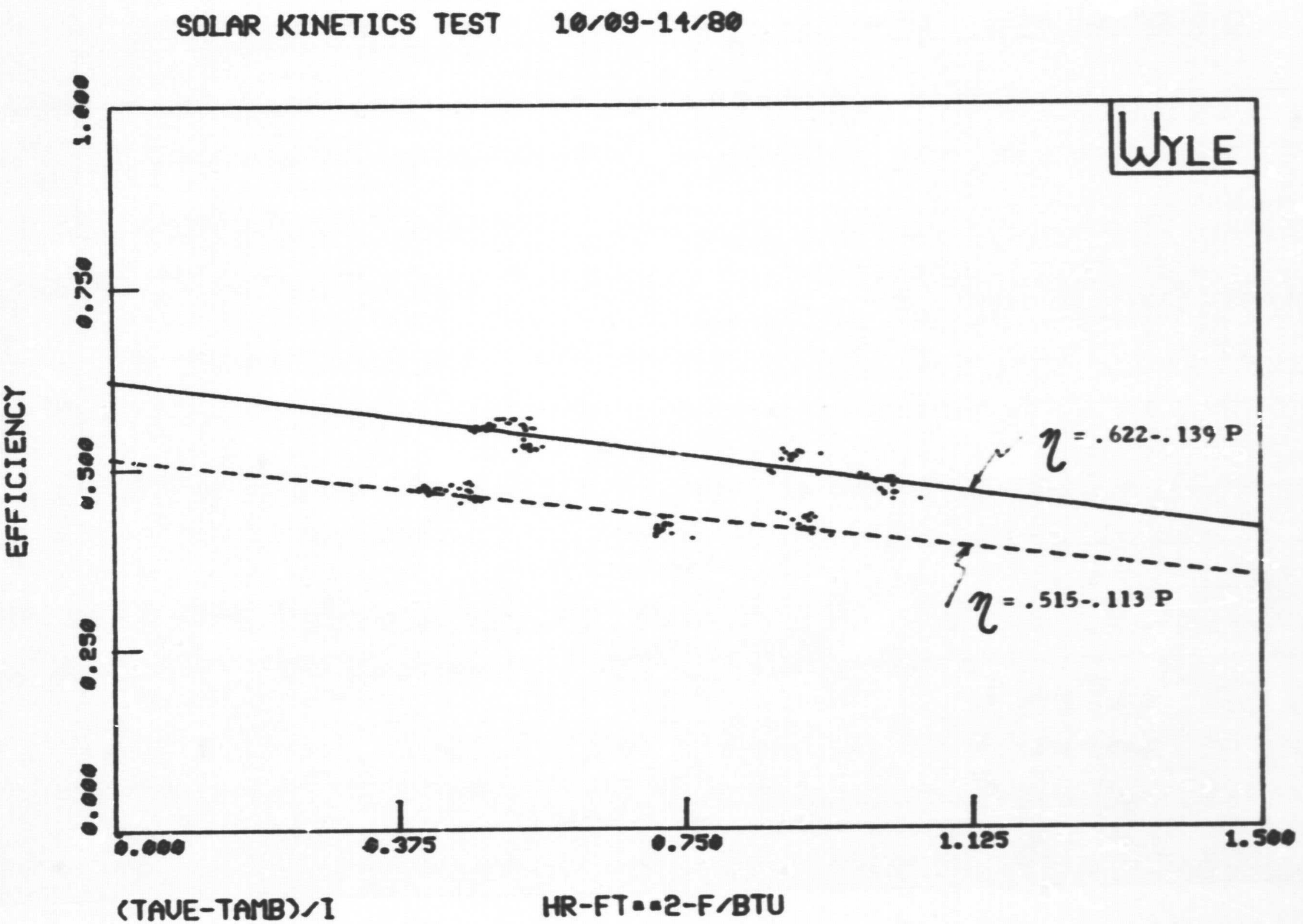

FIGURE 7. COLLECTOR THERMAL EFFICIENCY TEST AT HALF OF THE NORMAL FLOW RATE

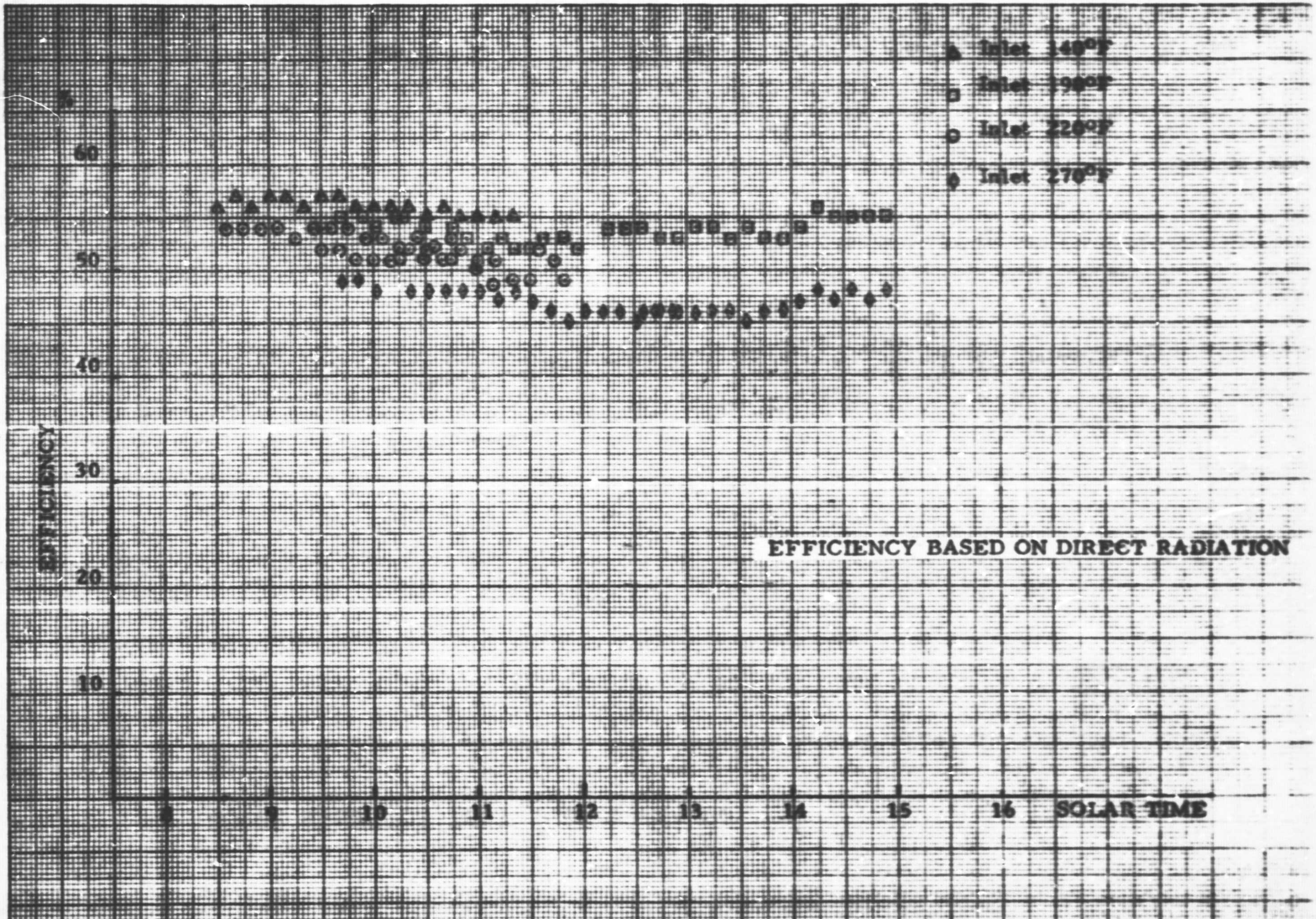

FIGURE 8. SOLAR KINETICS COLLECTOR ALL DAY TEST

ORIGINAL PAGE IS
OF POOR QUALITY

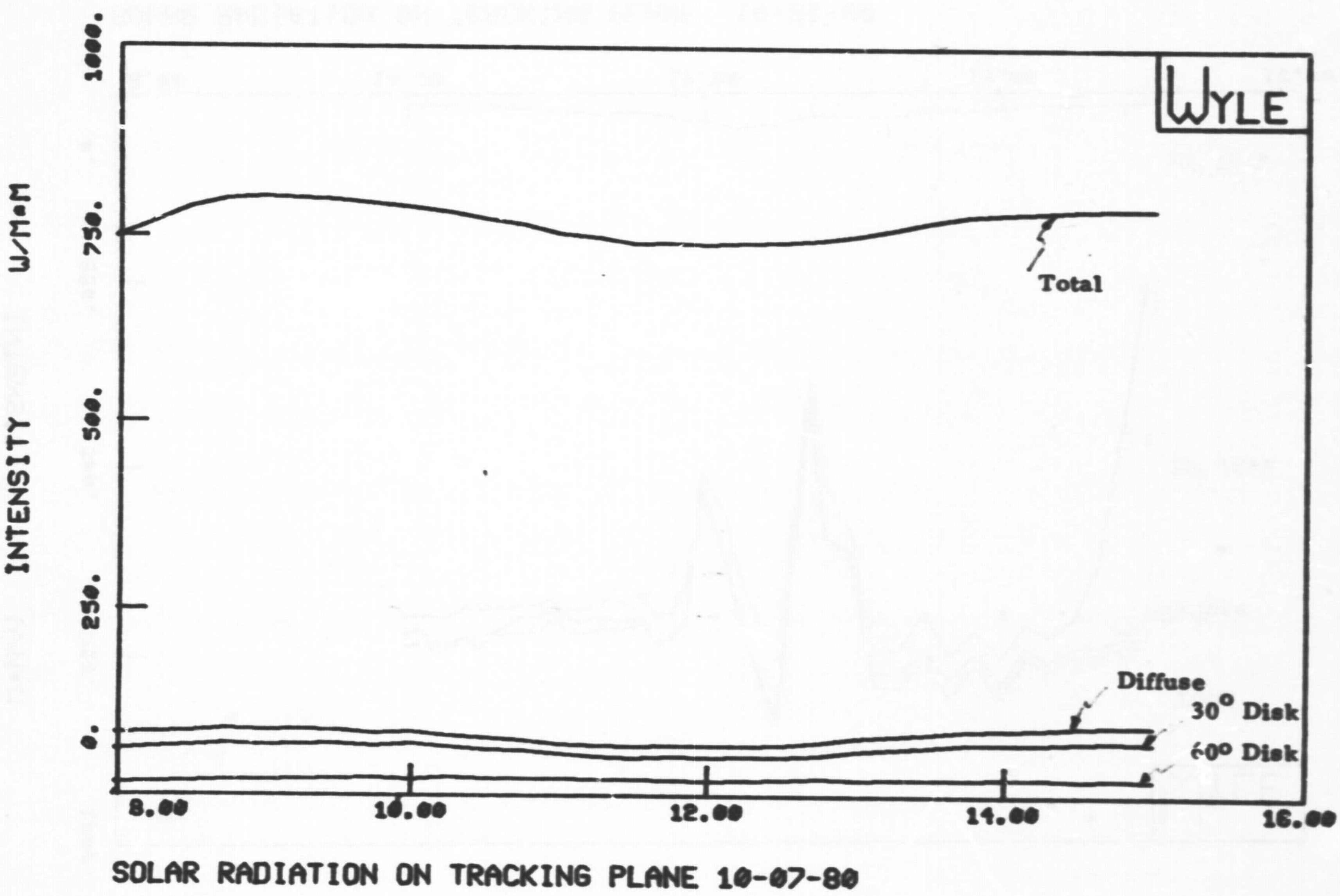

FIGURE 9. TYPICAL SOLAR RADIATION MEASUPED ON THE TRACKING PLANE

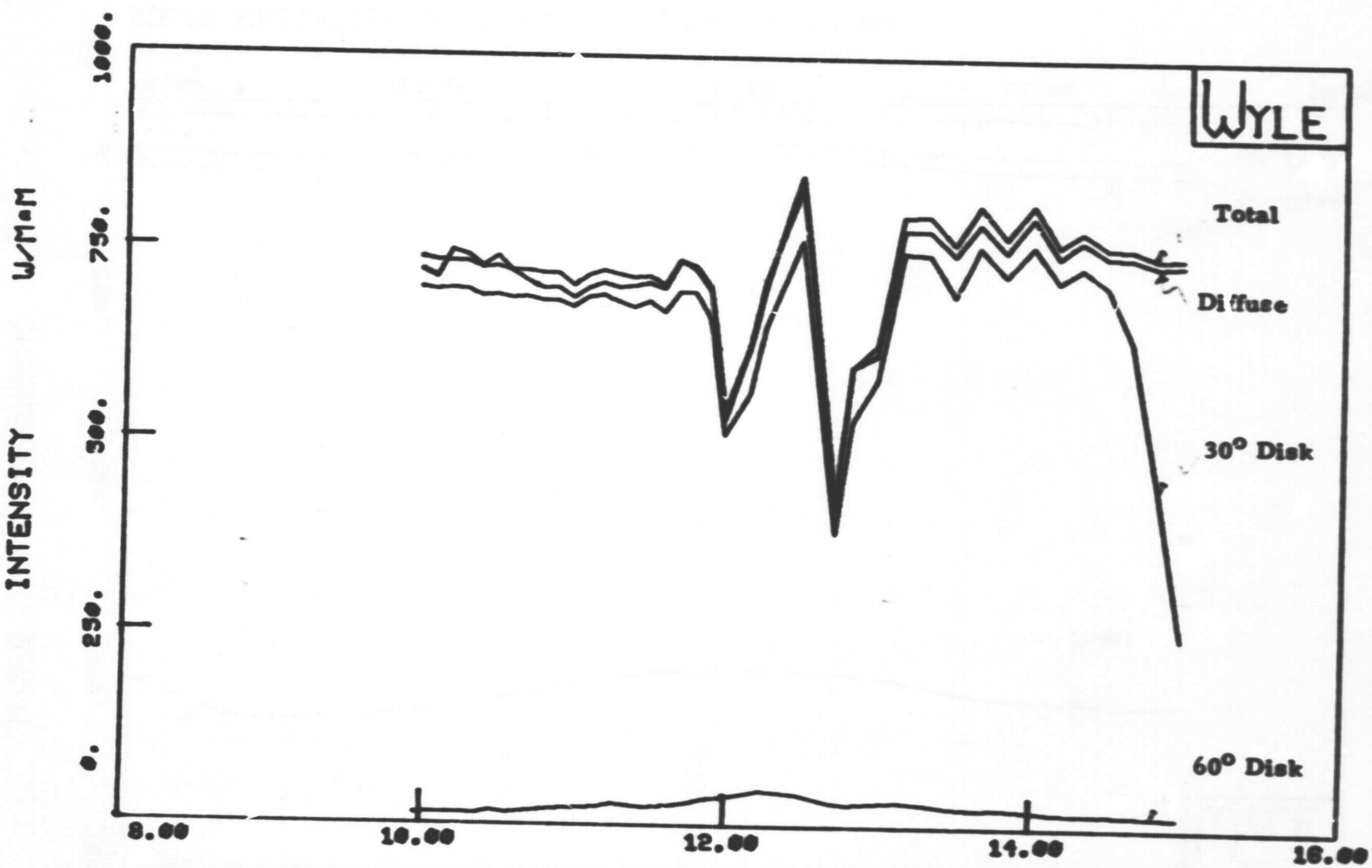

SOLAR RADIATION ON TRACKING PLANE 10-21-80

FIGURE 10. SOLAR RADIATION MEASURED ON THE TRACKING PLANE WHERE THE DIFFUSE AND 30° DISKS WERE NOT BLOCKING THE DIRECT SOLAR RADIATION

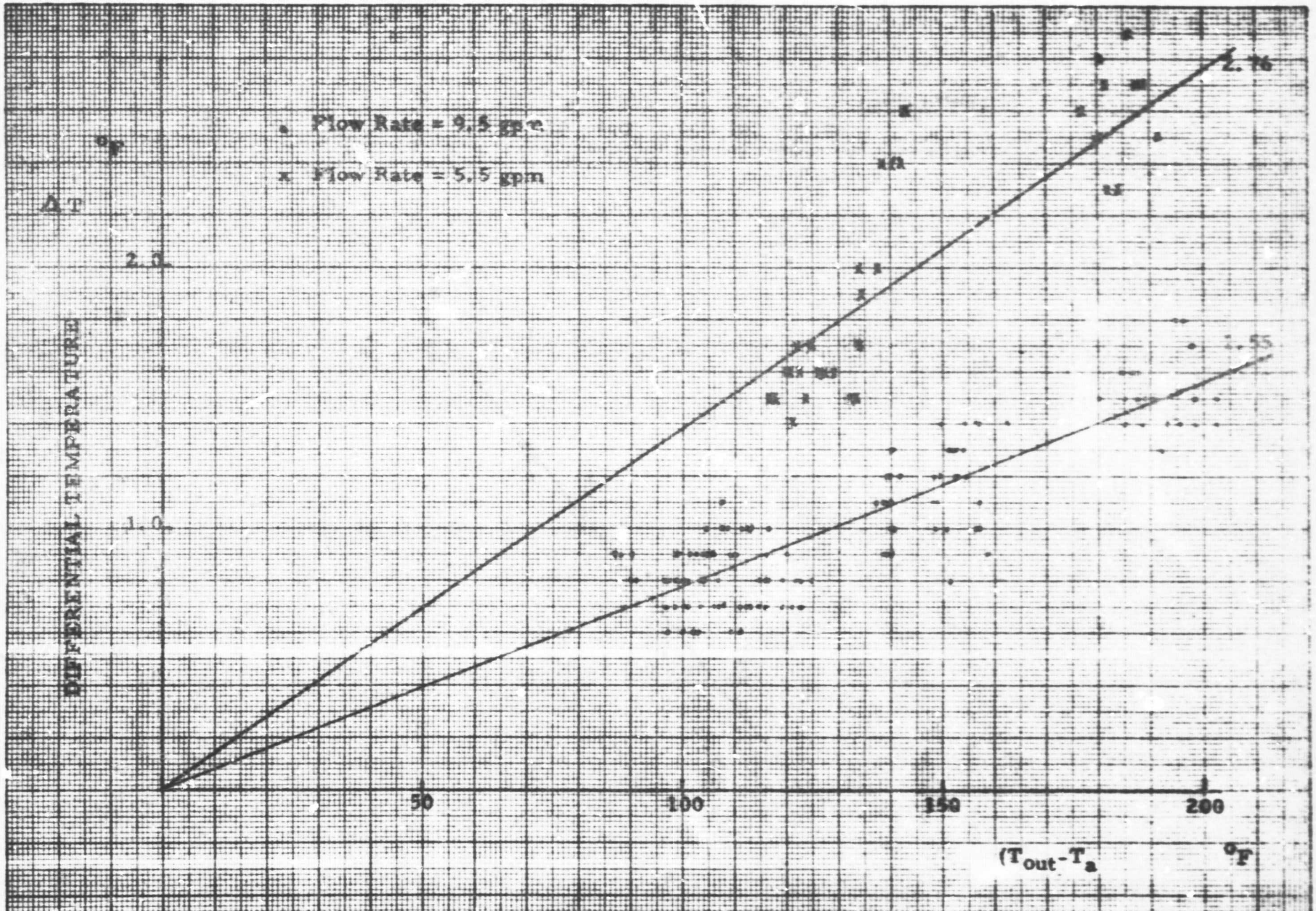

FIGURE 11. COLLECTOR RETURN LINE HEAT LOSS TEST

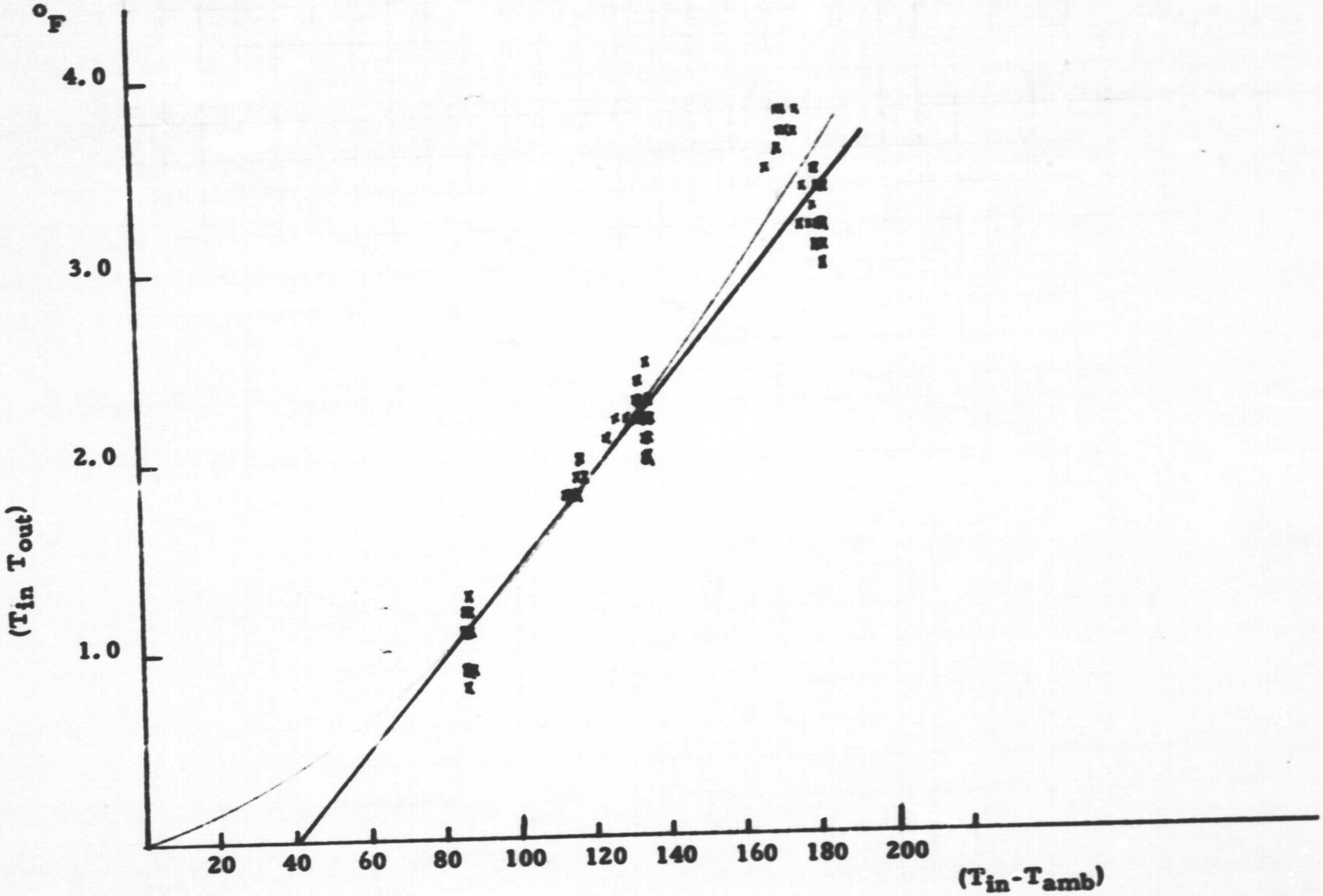

FIGURE 12. COLLECTOR ARRAY HEAT LOSS TEST

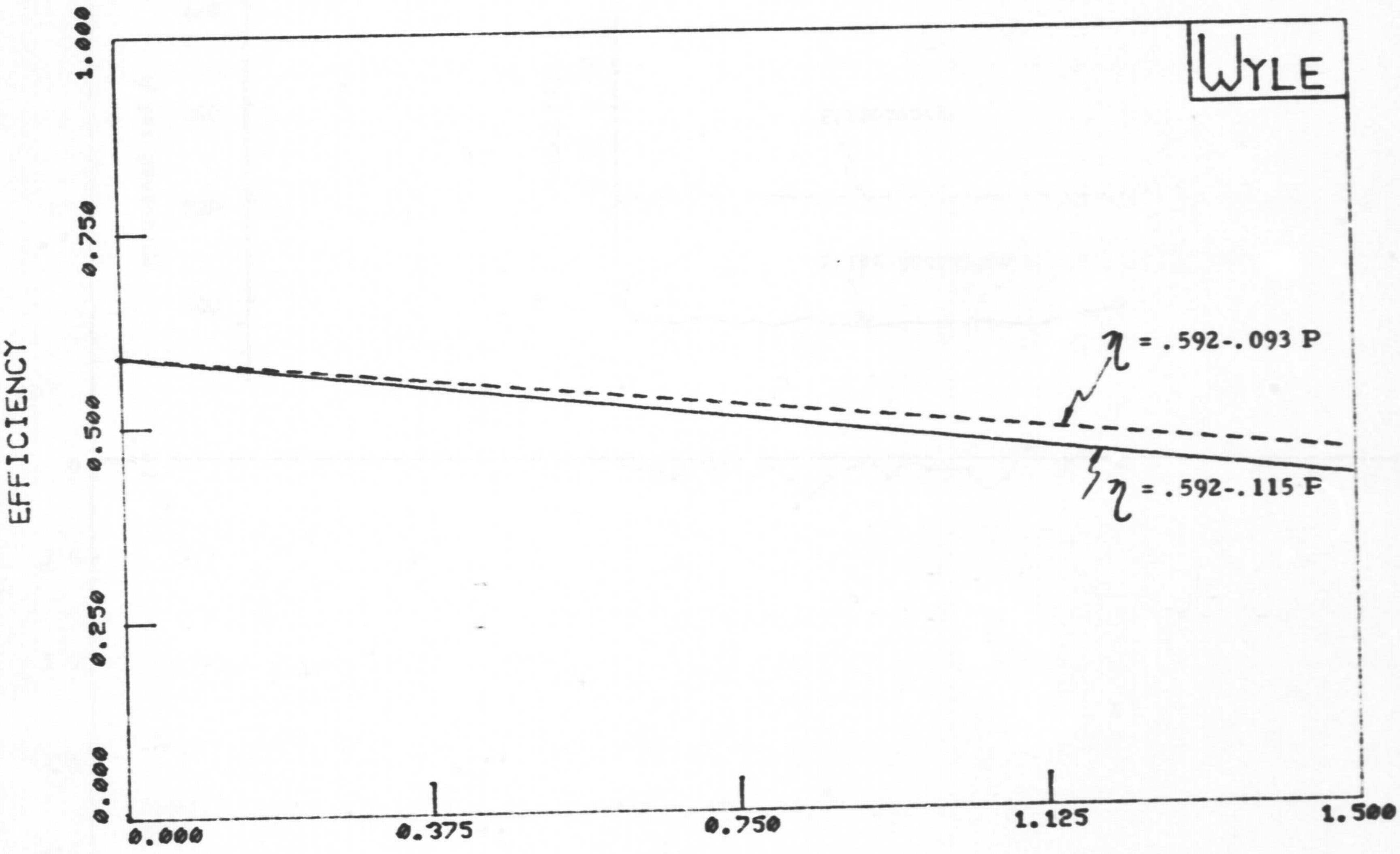

FIGURE 13. COMPARISON OF EFFICIENCY CURVE DERIVED FROM HEAT LOSS TEST WITH THE NORMAL THERMAL EFFICIENCY TEST

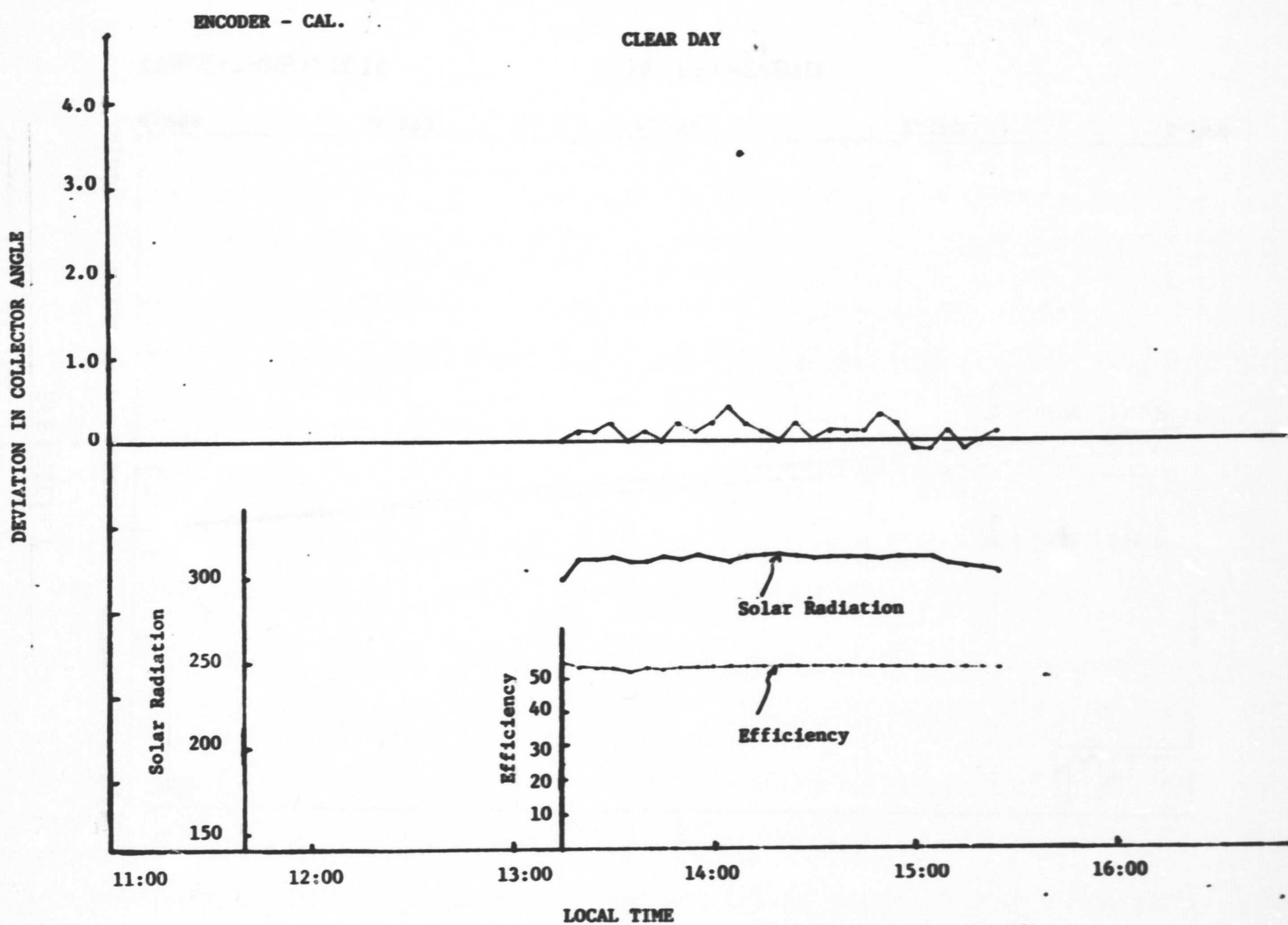

FIGURE 14. SOLAR KINETICS WITH SKI TRACKER ON A CLEAR DAY (6/18/81)

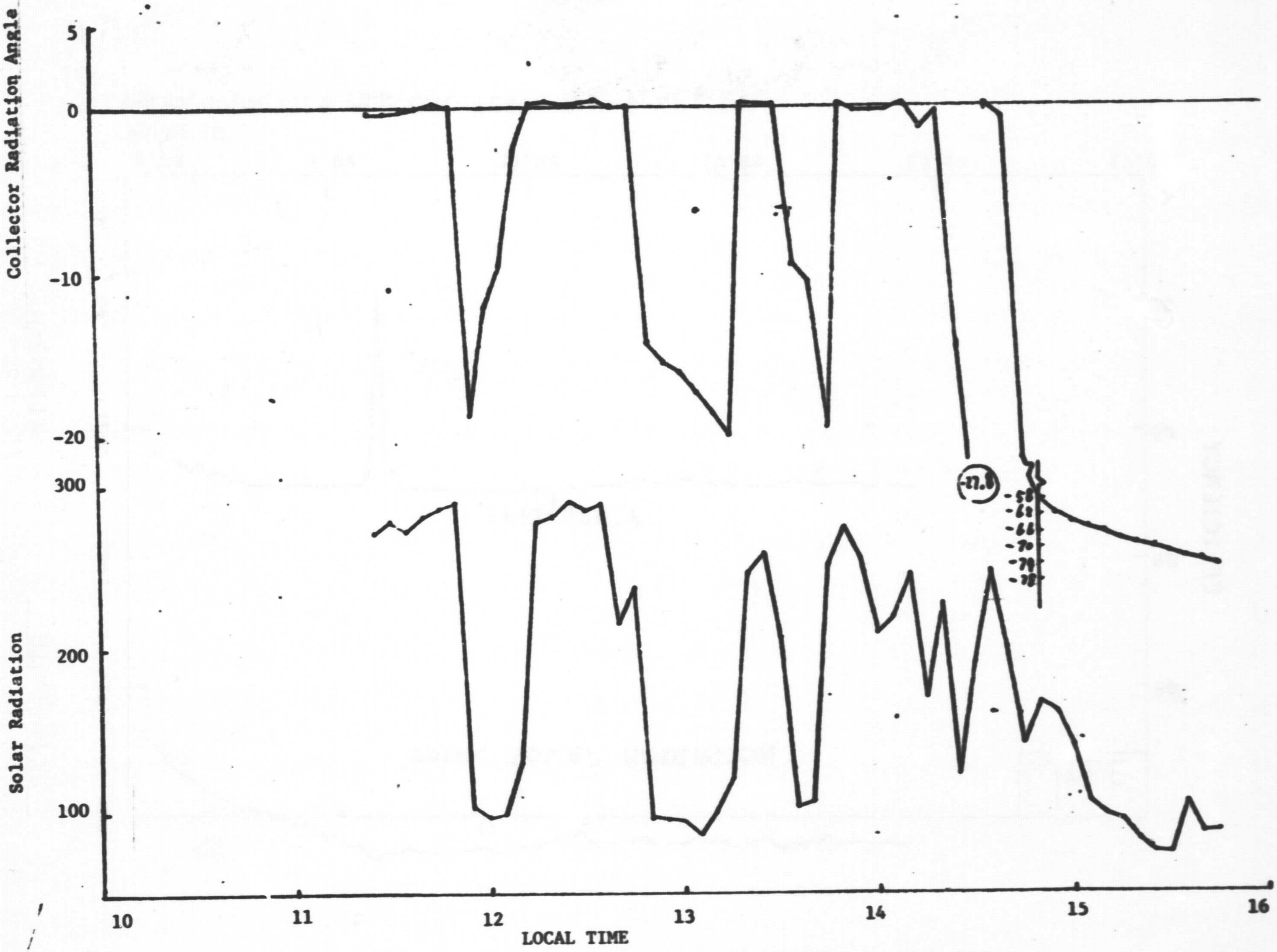

FIGURE 15. SOLAR KINETICS WITH SKI TRACKER ON AN INTERMITTENT DAY (8/14/81)

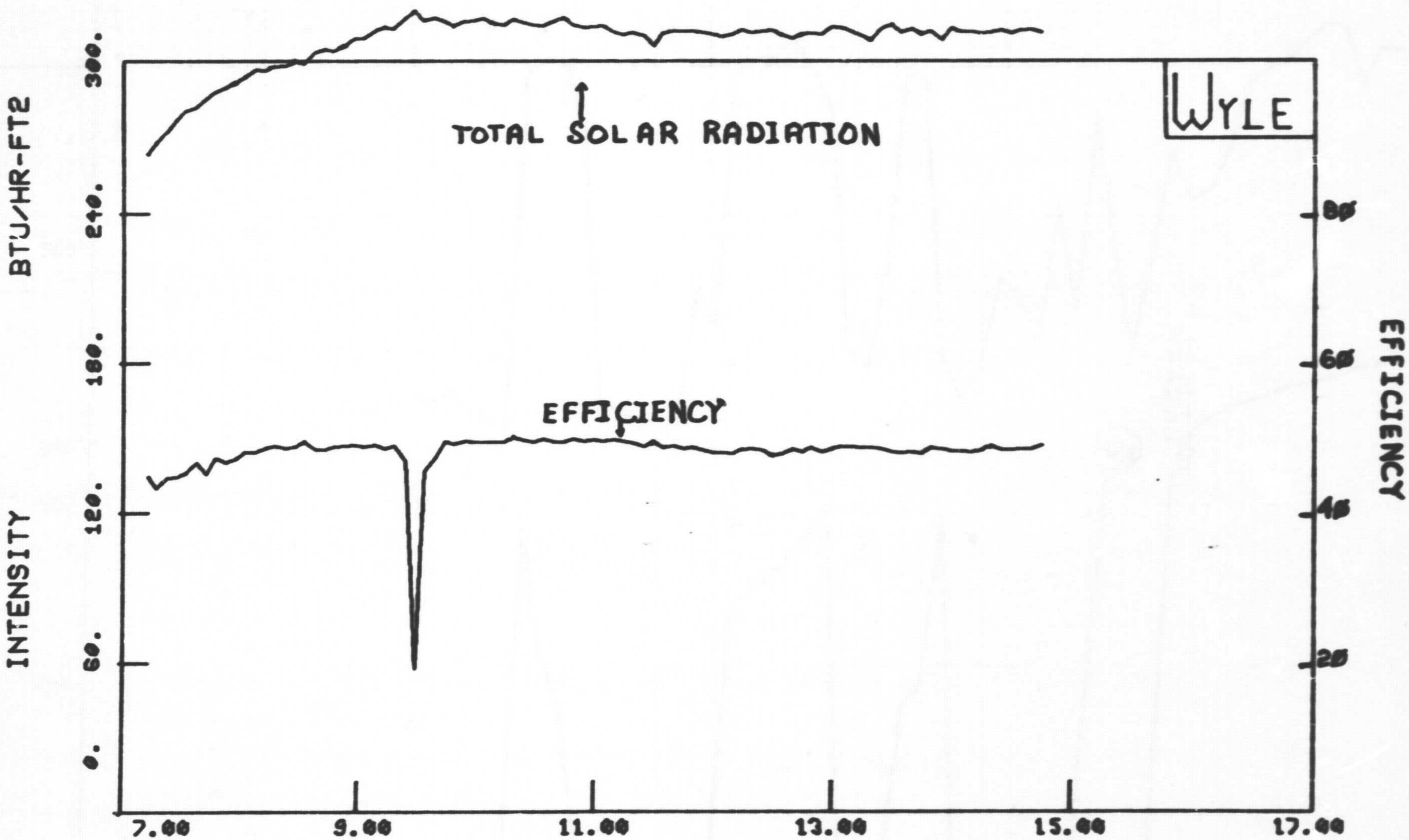

FIGURE 16.
SOLAR KINETICS ALL DAY TEST 6-26-1981

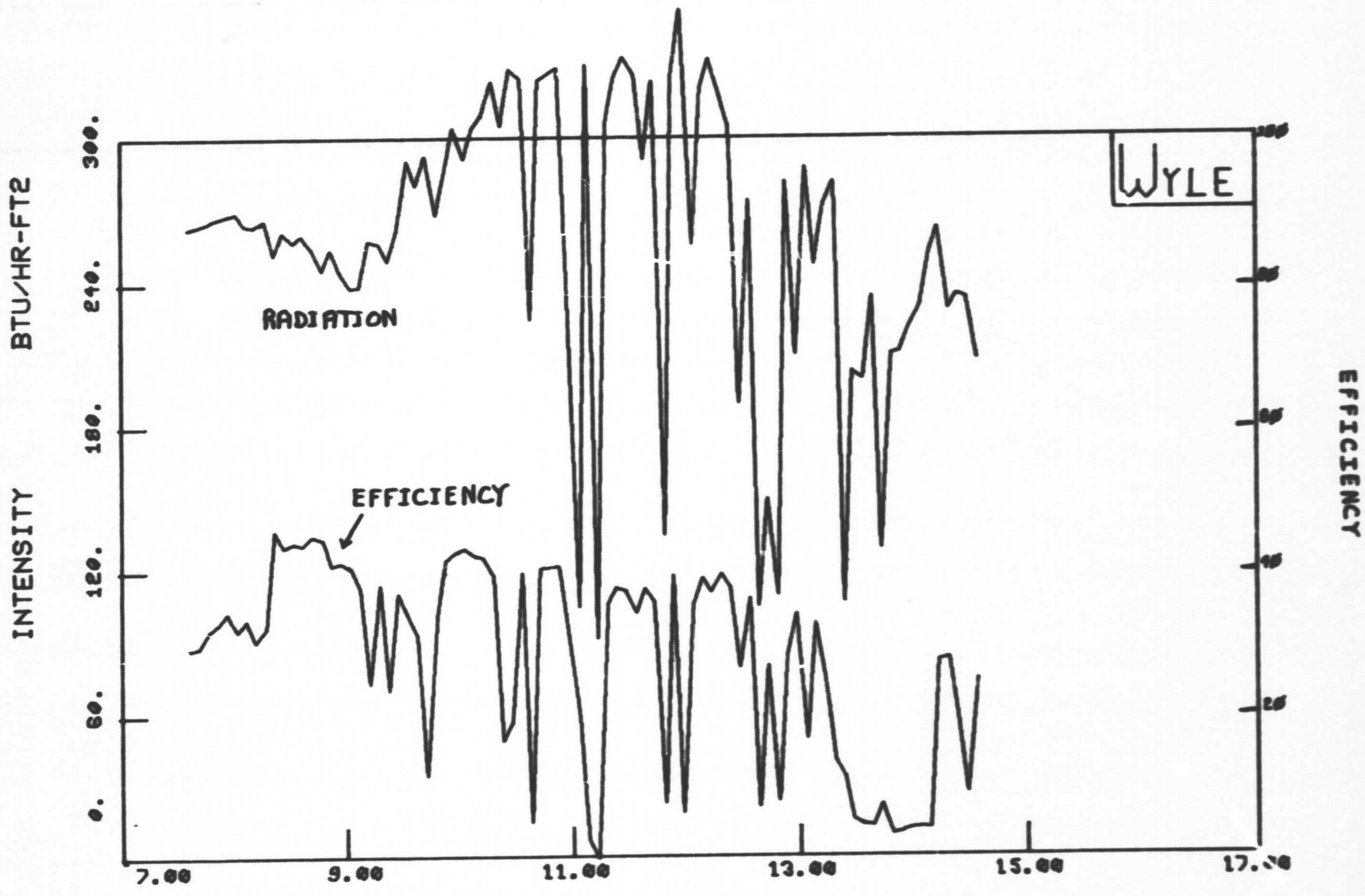

FIGURE 17.
SOLAR KINETICS ALL DAY TEST 7-7-1981